ADVANCED OPTICAL DIAGNOSTICS OF COLD ATMOSPHERIC PLASMAS IN RARE GAS JETS

João SANTOS SOUSA

***L**aboratoire de **P**hysique des **G**az et des **P**lasmas (**LPGP**)*

CNRS & Université Paris-Saclay

France

PLASMA JETS

All kinds of electrical excitations: DC, AC, RF, MW, continuous or pulsed

Rare gases (with or without admixtures: O_2, N_2, H_2O_2,…) but also pure N_2 or Air

Unlimited terminology: APPJ, Plasma Plume, Plasma Pencil, Plasma Gun, Plasma Torch,…

Discharge operated in a non-sealed electrode arrangement
plasma « expansion » outside the discharge region
either through high gas flow or determined by the electric field

Plasma or afterglow (effluent) delivery on targets


Osaka University

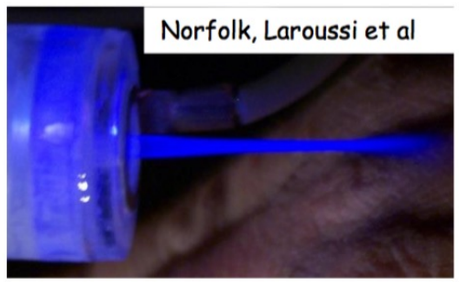

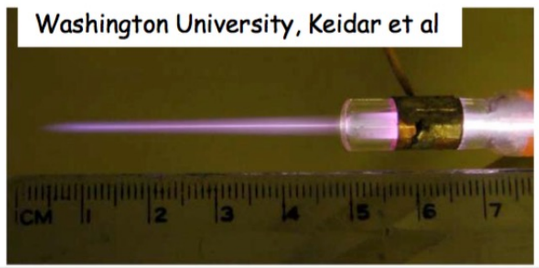

PSST 19 (2010) 025003
Z. Cao et al

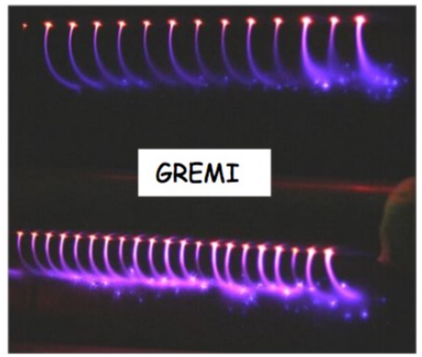

PLASMA JETS

DC microplasma

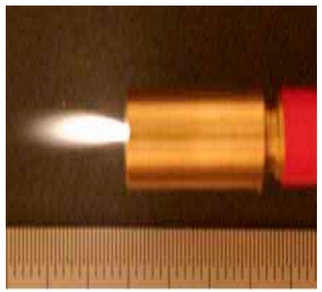

RF plasma jet

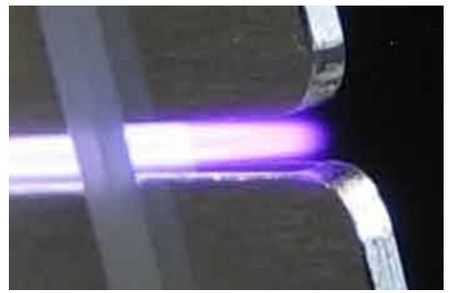

microwave

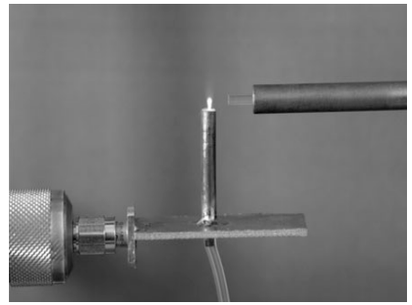

HV-LF excitation

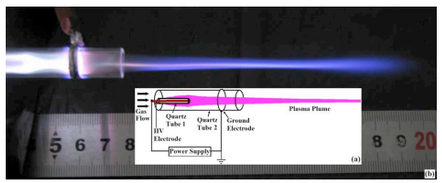

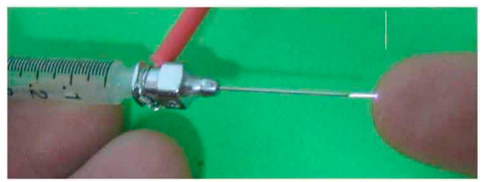

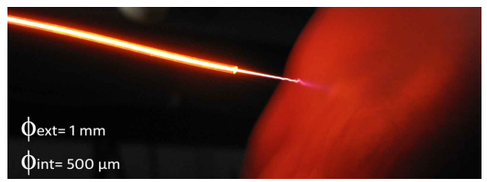

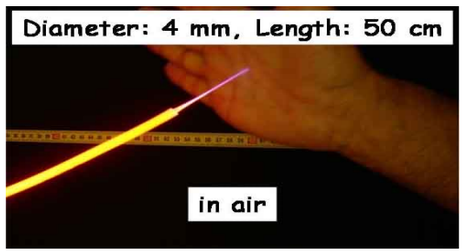

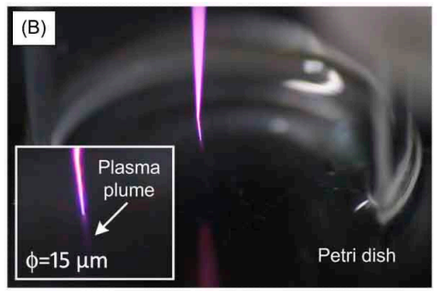

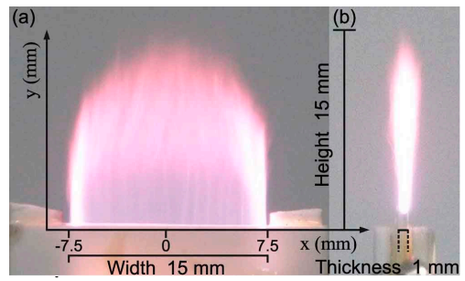

PLASMA JETS

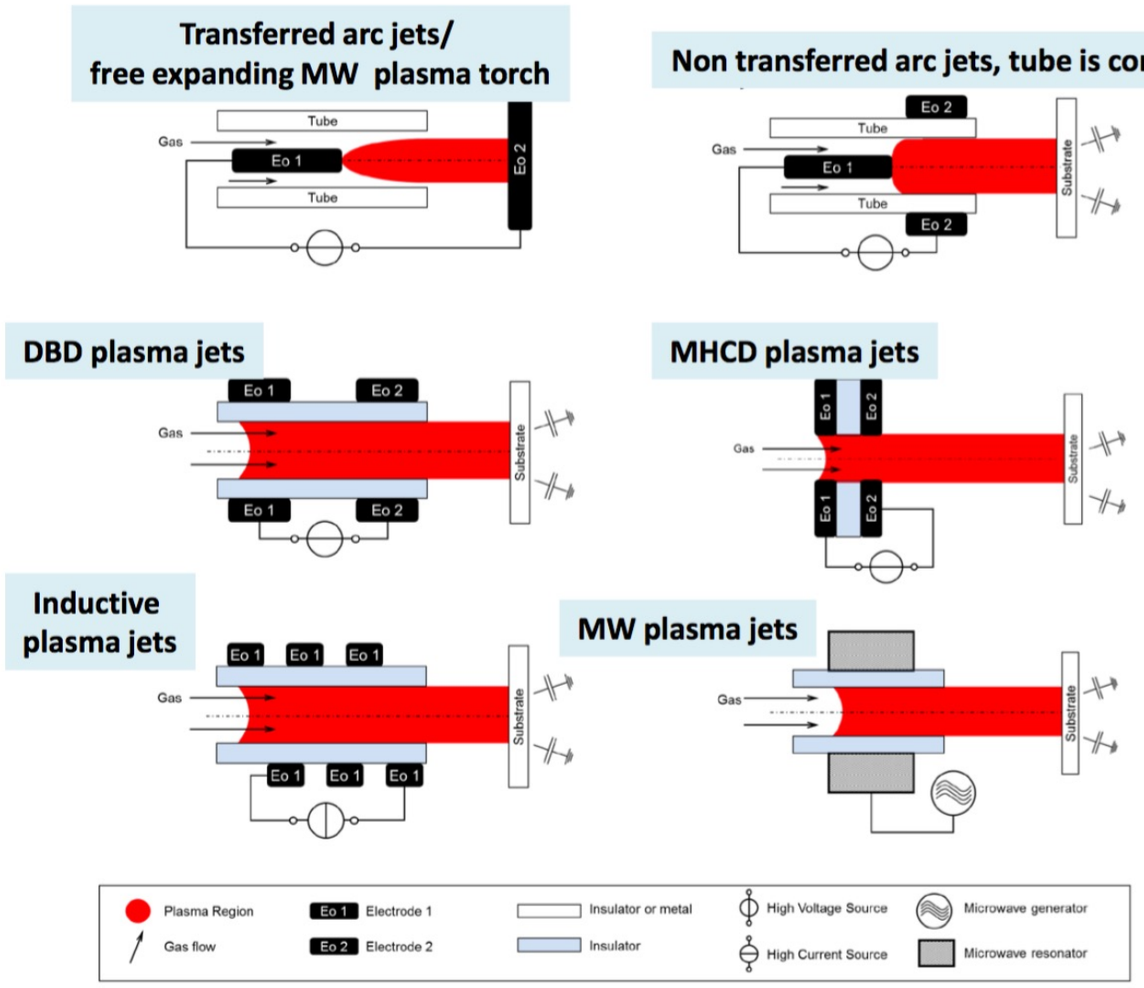

Cross sectional views of the basic geometries of coaxial plasma jets

Almost all well-known “old atmospheric pressure discharges” have been coined / called more recently as plasma jets!

J Winter *et al* Plasma Sources Sci. Technol. **24 (2015) 064001**

PLASMA JETS

Room-temperature atmospheric pressure plasma plume for biomedical applications

M. Laroussi[a] and X. Lu APPLIED PHYSICS LETTERS **87**, 113902 (2005)

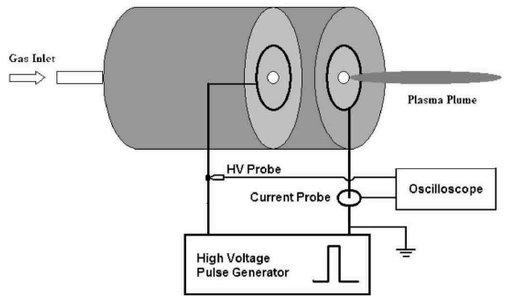

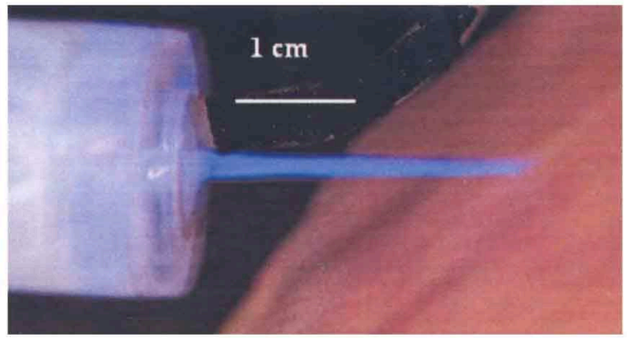

FIG. 2. (Color online) Photograph of the plasma plume in contact with human skin.

Dynamics of an atmospheric pressure plasma plume generated by submicrosecond voltage pulses

XinPei Lu and Mounir Laroussi[a] JOURNAL OF APPLIED PHYSICS **100**, 063302 (2006)

plasma pencil," is driven by few hundred nanosecond wide pulses at repetition rates of a few kilohertz. Correlation between current-voltage characteristics and fast photography shows that the plasma plume is in fact a small bulletlike volume of plasma traveling at unusually high velocities.

MICROPLASMA JET

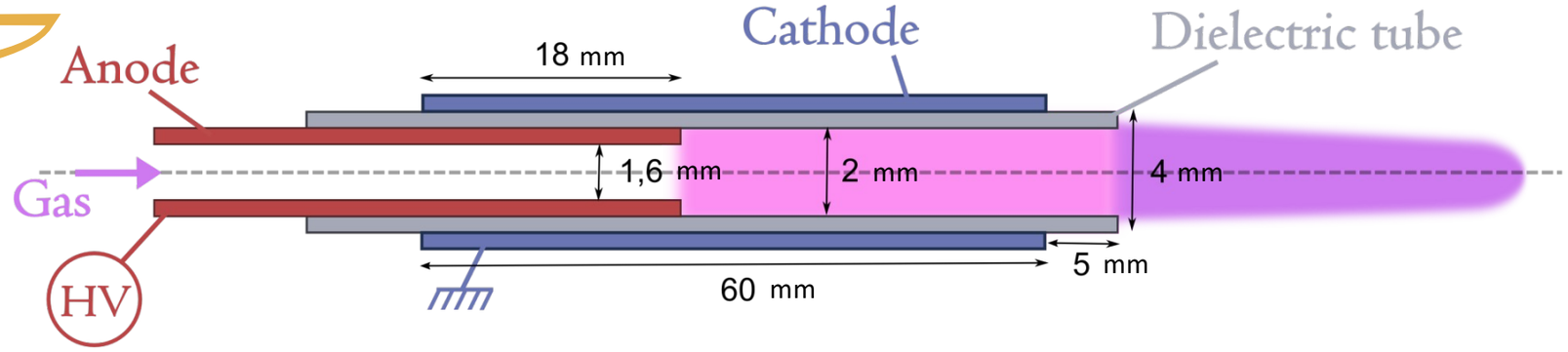

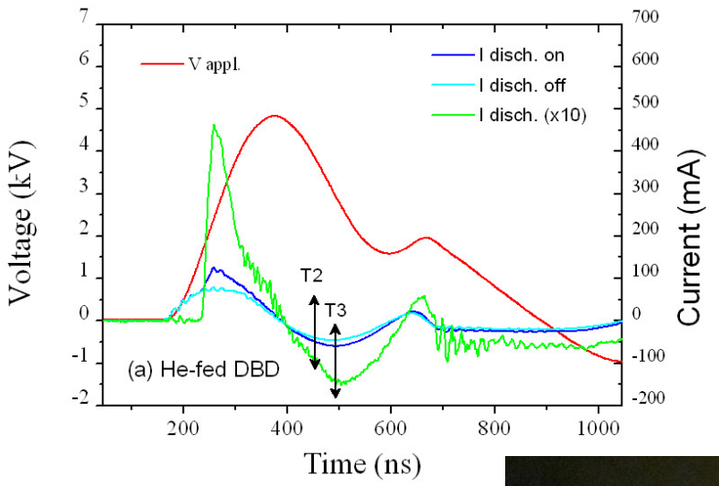

Coaxial DBD

Applied voltage (pulsed) : **3–40 kV (100ns–10µs)**
(typically 6 kV, 500 ns)

Frequency : **1–50 kHz** (typically 20 kHz)

Gas : **He, Ar, with or without O_2/N_2/H_2O**

Gas flow : **50 to 5000 sccm**

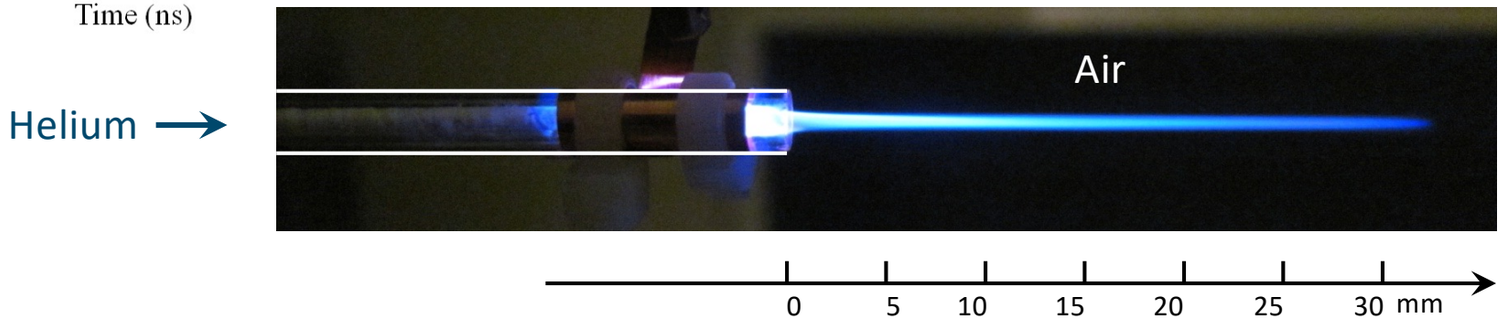

MICROPLASMA JET

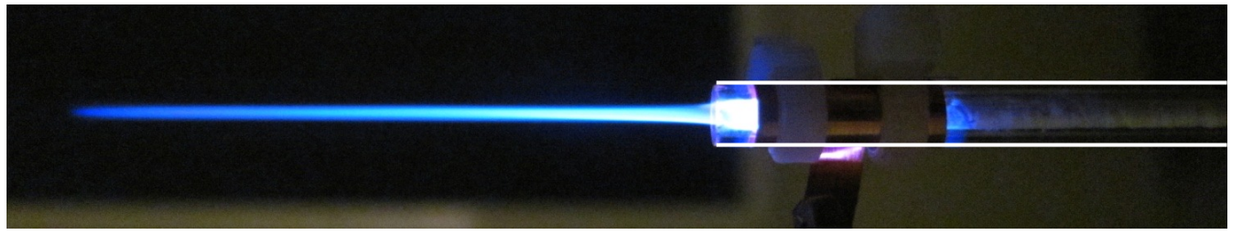

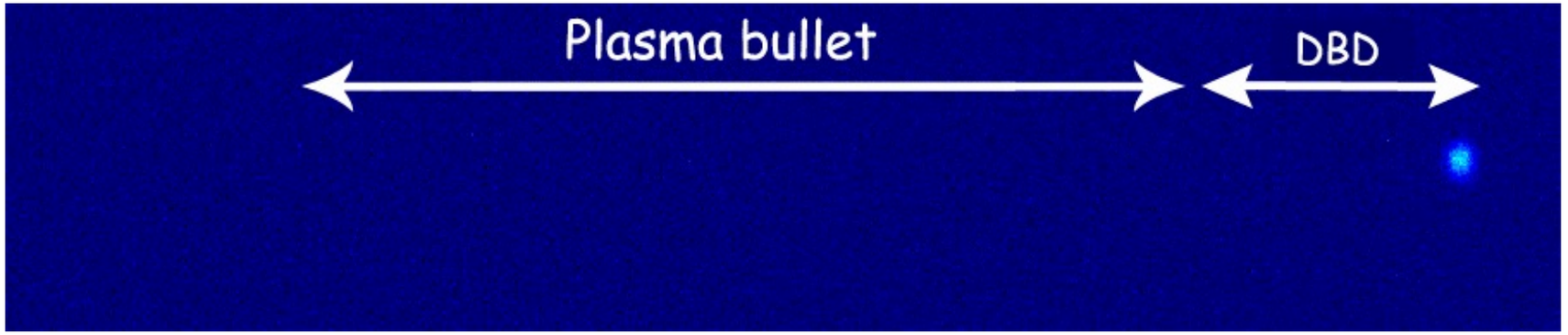

The plasma jet is not continuous; it is rather a streamer guided by the gas channel

The velocity of the “guided streamer” is of several hundreds km/s

Stable at atmospheric pressure
Low gas temperature ≈ 300-350 K

ENDOSCOPIC TREATMENTS

Possible use for endoscopic treatments

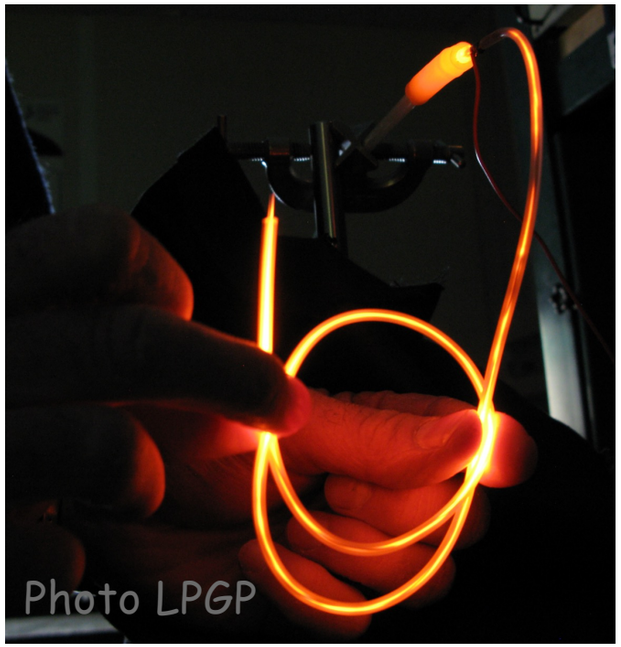

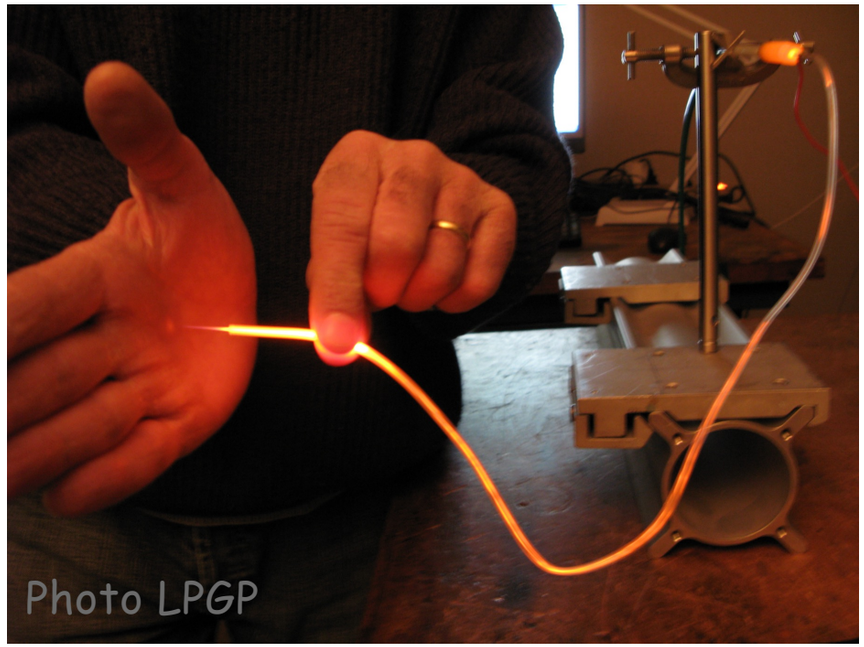

Periodic forced flow in a ns-pulsed cold atmospheric pressure argon plasma jet

Thibault DARNY,

Gérard BAUVILLE, Michel FLEURY, Stéphane PASQUIERS and João SANTOS SOUSA

Laboratoire de Physique des Gaz et des Plasmas (LPGP)
CNRS & Université Paris-Saclay
Orsay, France

INTRODUCTION

Cold atmospheric pressure plasma jets (CAPPJ) : ➡ Biomedicine ➡ Depollution ➡ Decontamination ➡ Analytical chemistry ➡ Material processing

K Gazeli *et al.* 2020 J. Phys. D: Appl. Phys. 53 475202

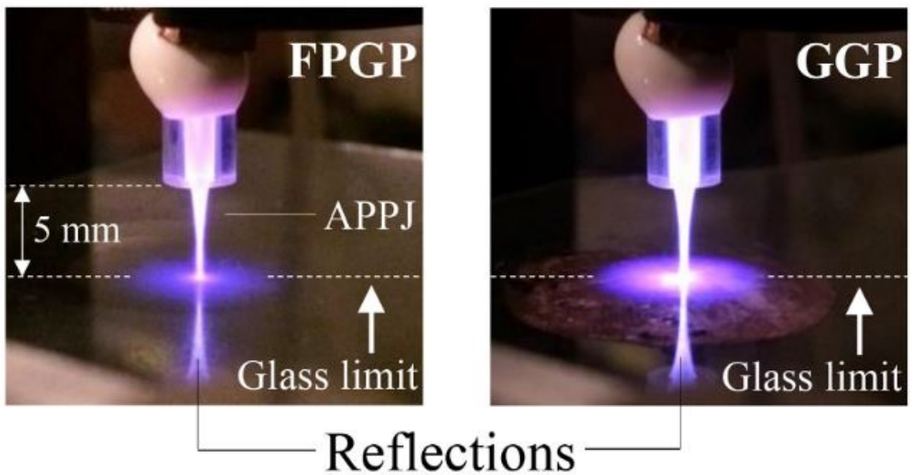

fast desorption of weakly volatile organic compounds deposited on glass substrates

H Nizard *et al.* 2015 J. Phys. D: Appl. Phys. 48 415204

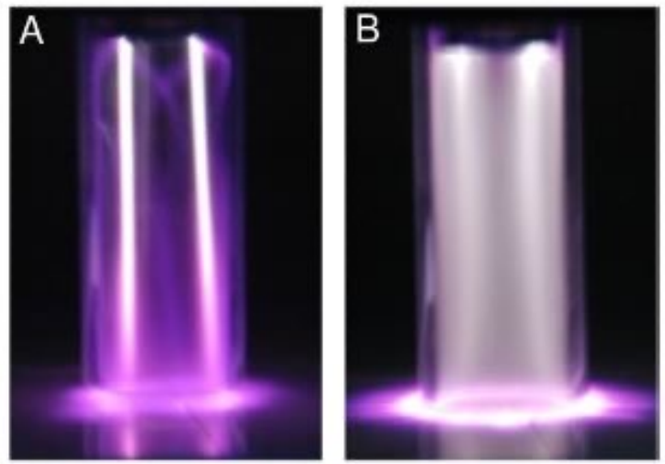

Influence of discharge and jet flow coupling on atmospheric pressure plasma homogeneity

Reactive species production and surface interaction are strongly influenced by the mixing with ambient air

INTRODUCTION

➡ **Flow modification: more studies on helium CAPPJ than on argon CAPPJ**

Argon jets : Only RF and microwave

Zhang *et al.* J. Phys. D: Appl. Phys. 48 (2015) 015203

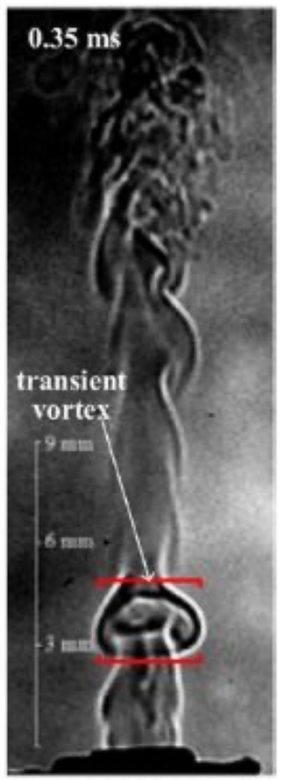

≠

Helium jets: DC pulsed and AC

Morabit *et al.* Plasma Process Polym. 2020;17:e1900217

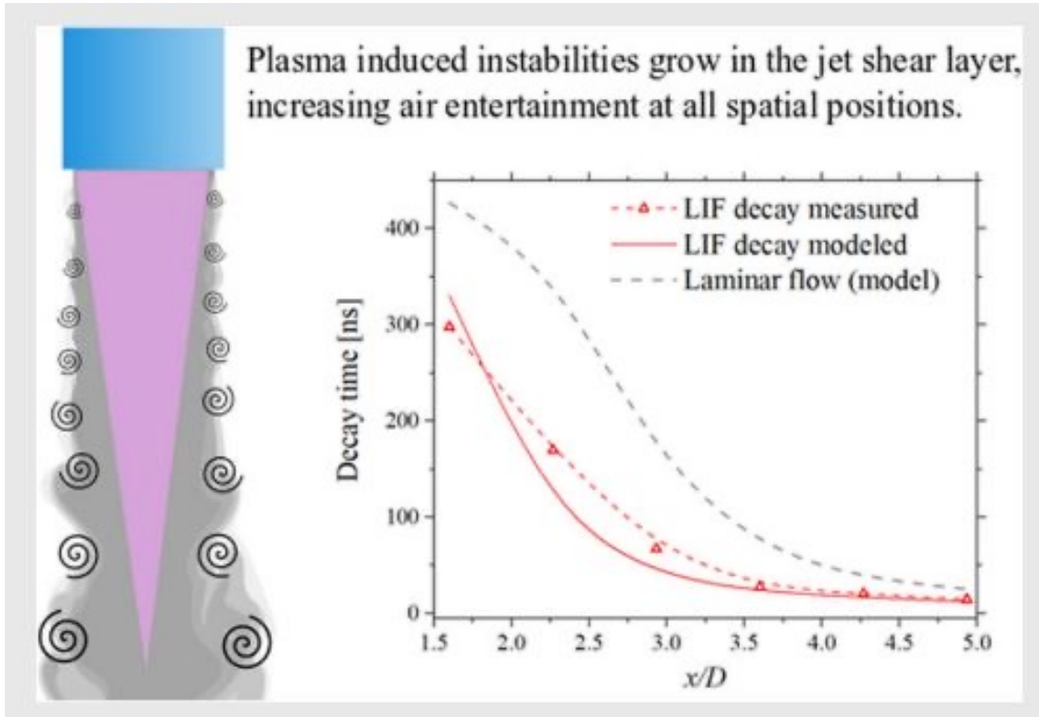

➡ **Significant gas heating due to plasma power**

In the plasma plume

➡ **gas heating is negligible**

➡ **flow velocity increase is negligible**

➡ **ionic wind is negligible**

INTRODUCTION

➡ **Helium CAPPJ with one High Voltage (HV) pulse application**

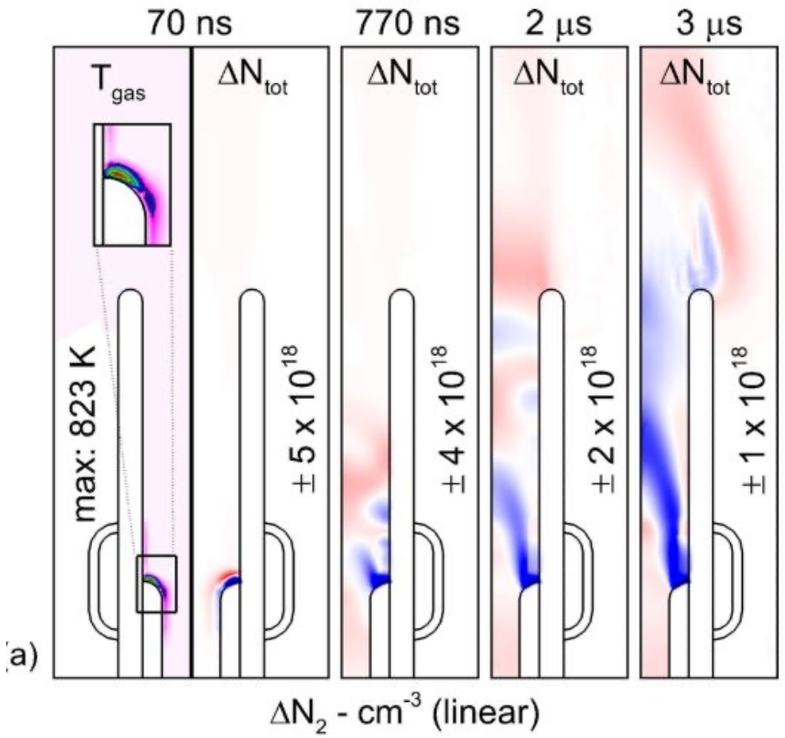

Lietz, Johnsen, and Kushner
Appl. Phys. Lett. 111, 114101 (2017)

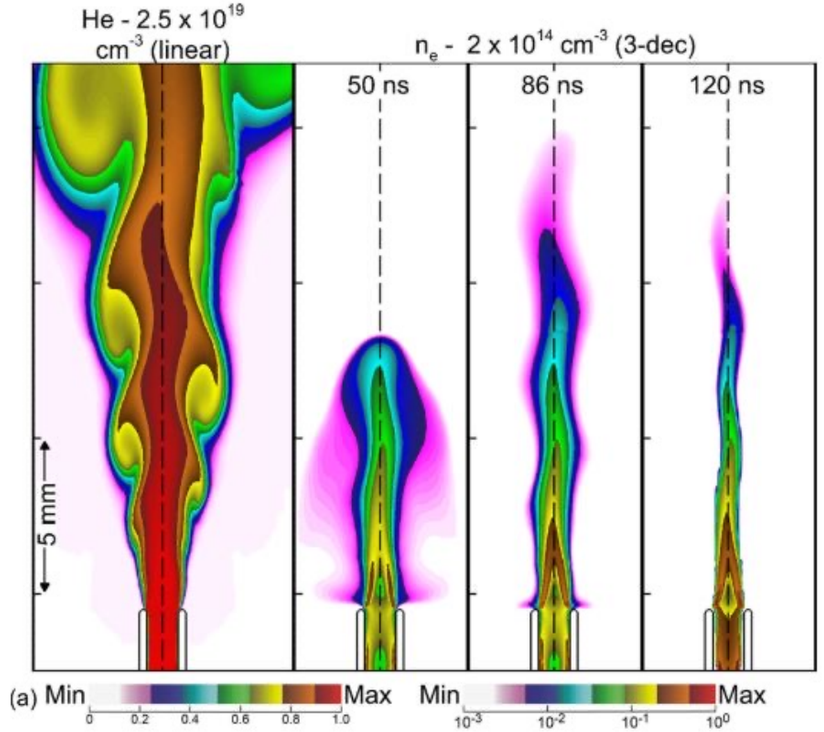

➡ **Ionization wave ignition at the inner HV electrode inside the capillary**

➡ **Local ultra-fast gas heating**

➡ **Pressure increases by a factor 2**

➡ **Pressure wave excites the highly unstable helium shear layer**

Up to now, no comparable studies with argon CAPPJ powered by DC pulses

EXPERIMENTAL SETUP

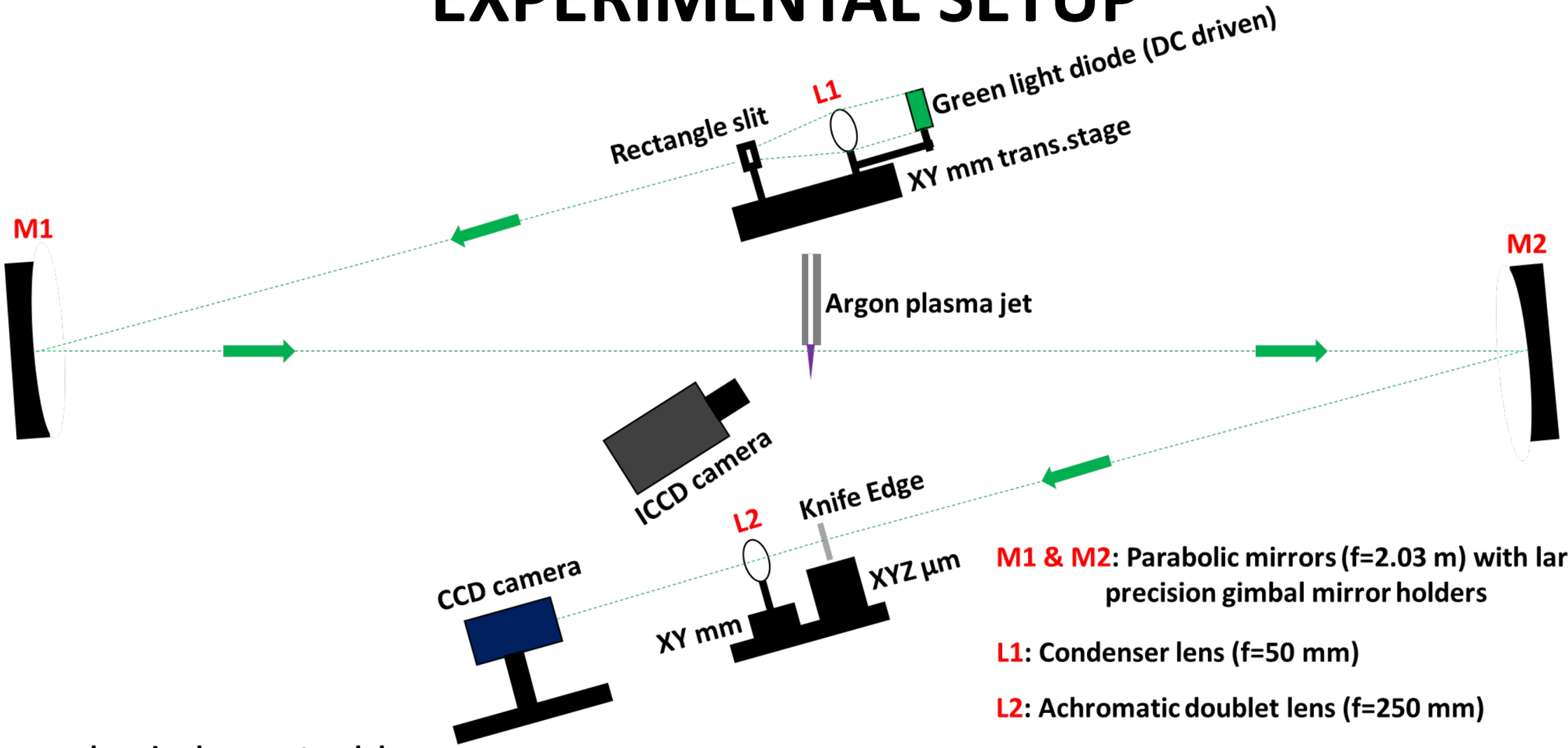

M1 & M2: Parabolic mirrors (f=2.03 m) with large precision gimbal mirror holders

L1: Condenser lens (f=50 mm)

L2: Achromatic doublet lens (f=250 mm)

two synchronized generator delays

- high voltage pulse sequences in burst mode
- image acquisition by CCD and ICCD

Flow rate range : 800 sccm to 400 sccm (100 sccm step)

EXPERIMENTAL SETUP

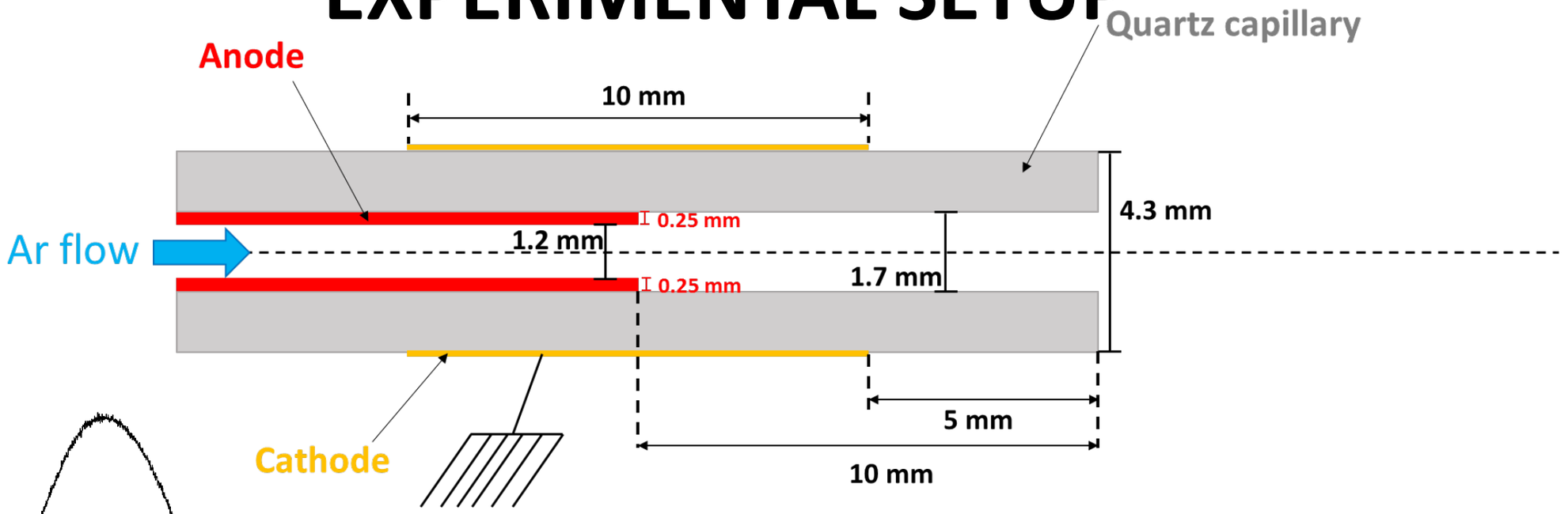

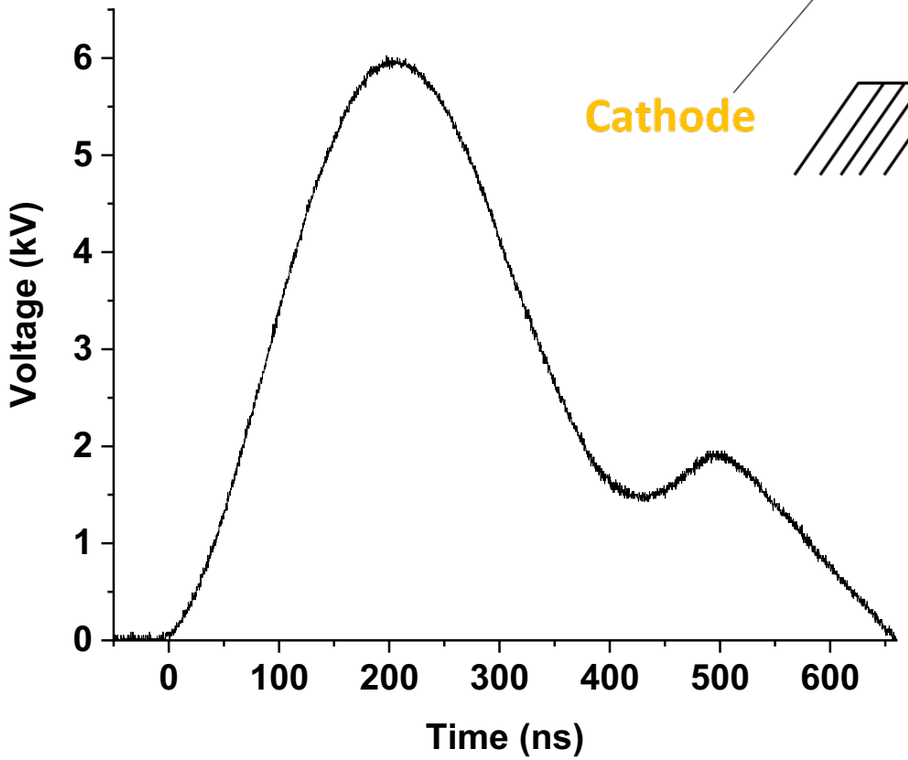

For each burst event

- Delay of the first High Voltage (HV) pulse
- Number of HV pulses
- Pulse repetition frequency (PRF)

The burst cycle is repeated 20 times with a 2 Hz frequency

For each conditions: 20 schlieren images and 20 ICCD images

Plasma OFF

Schlieren images (int: 1.446 ms)

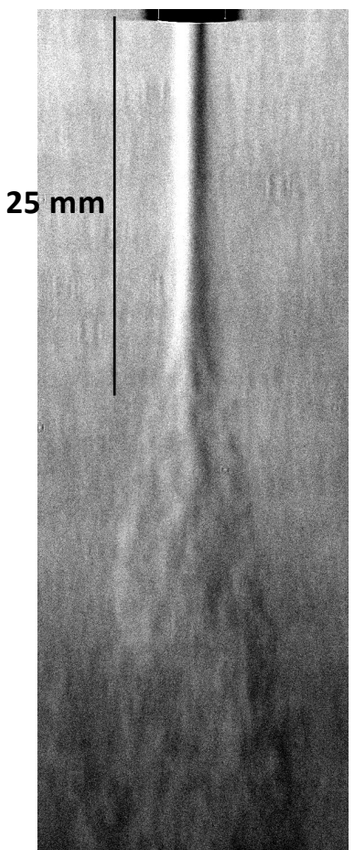

800 sccm flow rate

➡ Turbulent transition point : $\mathbf{23.7 \pm 1.6\ mm}$

Plasma OFF

Schlieren images (int: 1.446 ms)

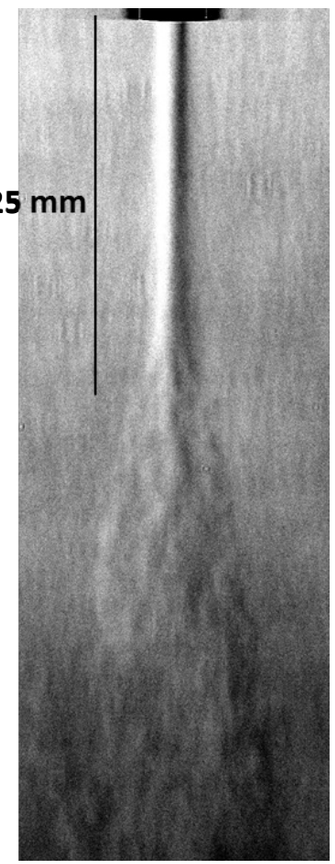

Single HV shot

ICCD images (int: 500 ns)

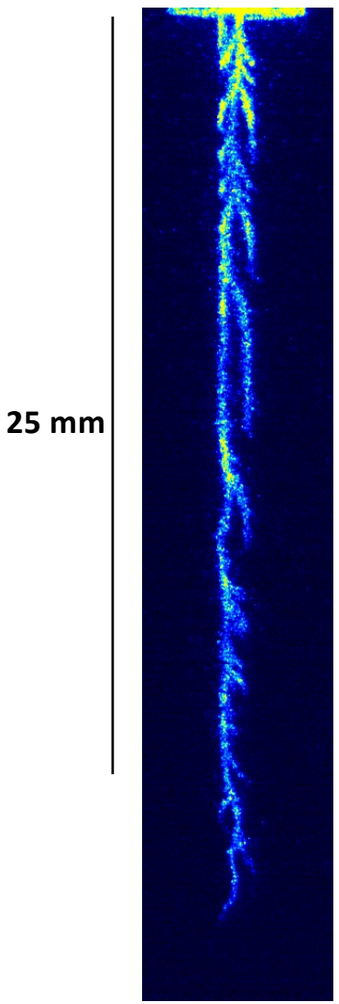

Single HV shot

numerical accumulation

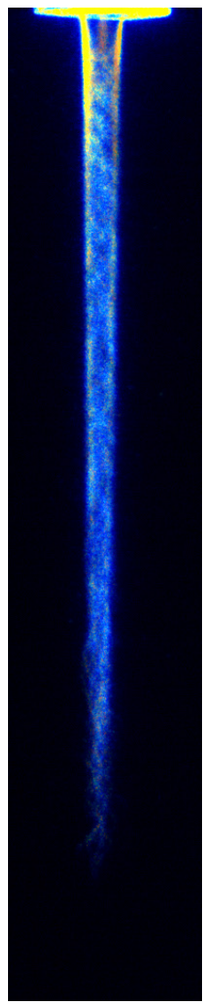

800 sccm flow rate

- Turbulent transition point : $\mathbf{23.7 \pm 1.6\ mm}$
- Plasma plume length : $\mathbf{25.6 \pm 2.2\ mm}$

Mean flow velocity : **11.8 m/s** **(Re=1241)**

Ionization wave (IW) propagation velocity : **~10^5 m/s**

During **500 ns** : fluid particles have only propagated on **6 µm**

On the timescale of IW propagation, the flow is static

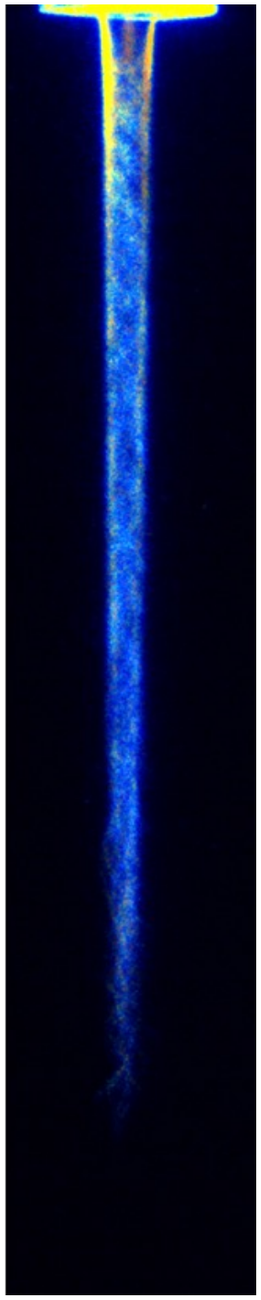

- IW **propagates inside the argon potential core**
- Static flow during IW propagation

A second IW can be used to probe the flow structure any time after the first HV pulse application

Δt= x ms

(time delay between the two HV shots)

First HV shot ⟷ **Second HV shot**

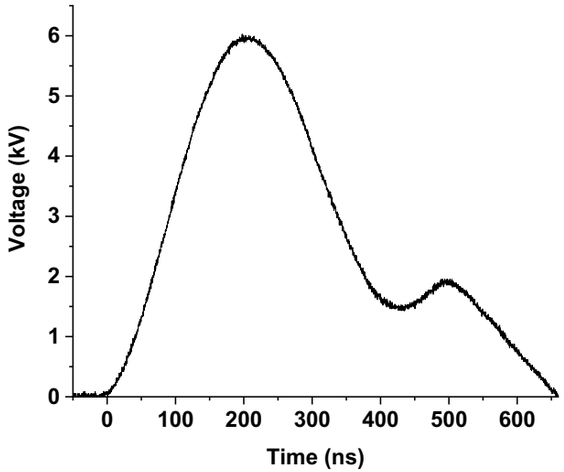

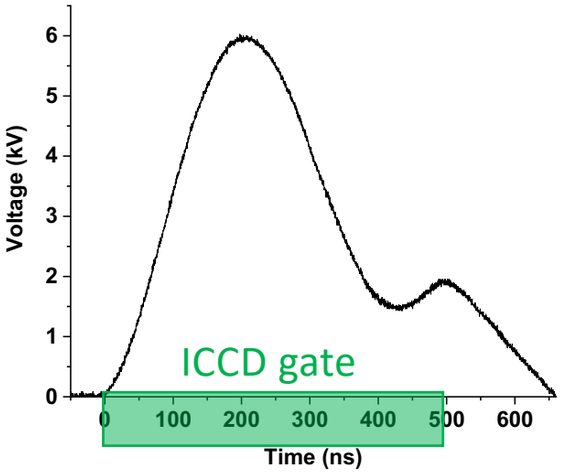

Double HV shots technique

Double HV shots

Δt = 0.90ms

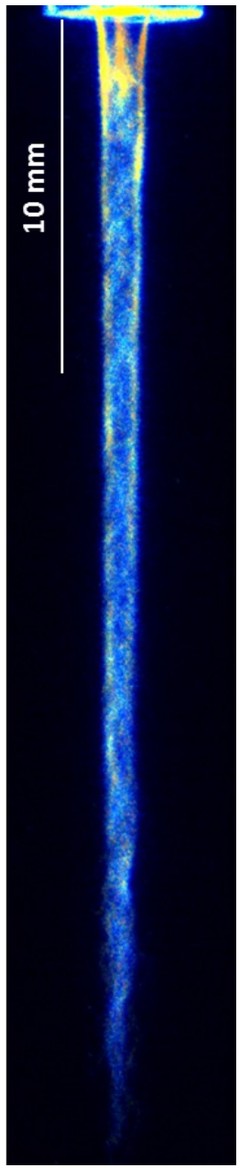

Double HV shots

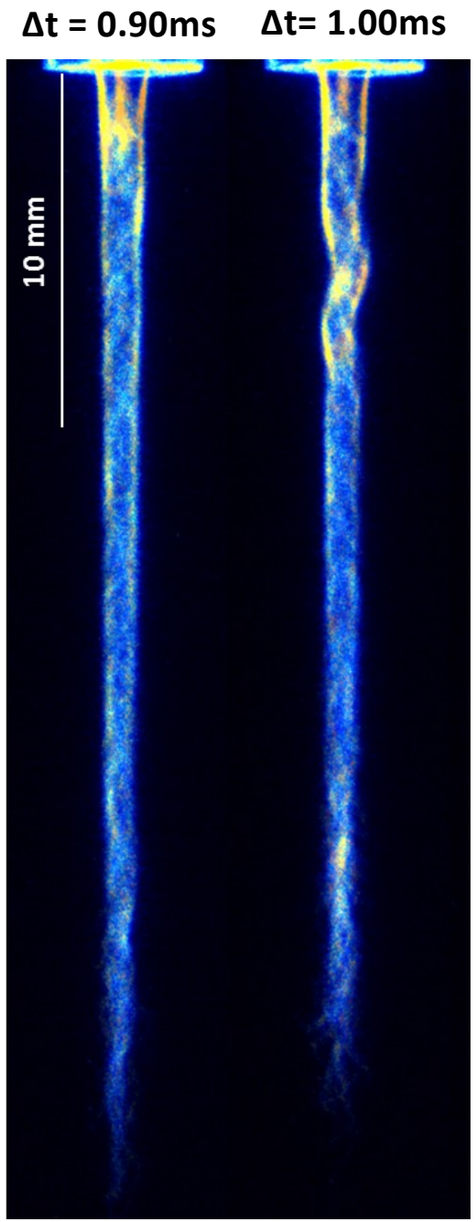

Double HV shots

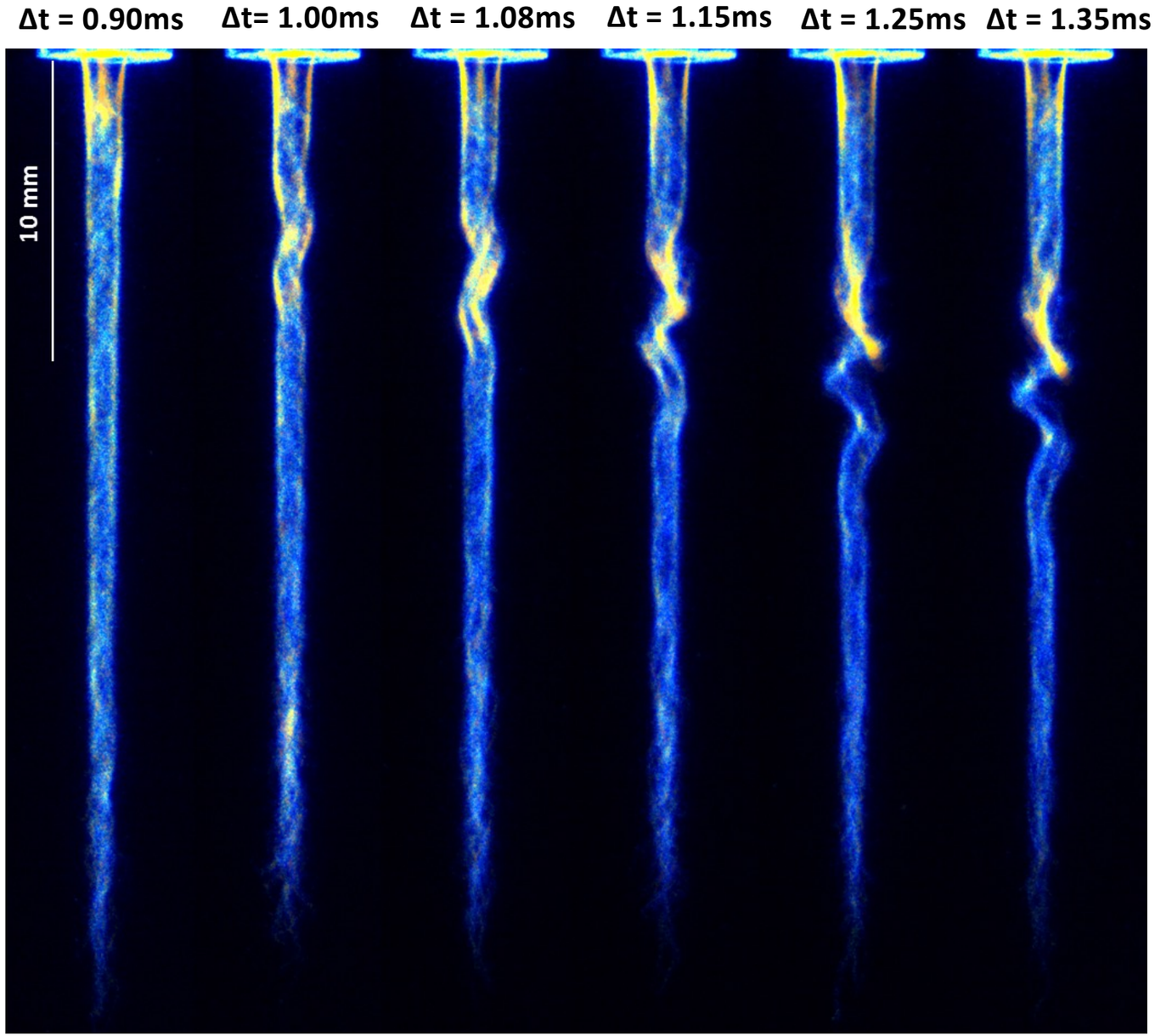

ripple with brightest plasma emission

Double HV shots

Δt = 0.90ms Δt= 1.00ms Δt = 1.08ms Δt = 1.15ms Δt = 1.25ms Δt = 1.35ms Δt = 1.45ms

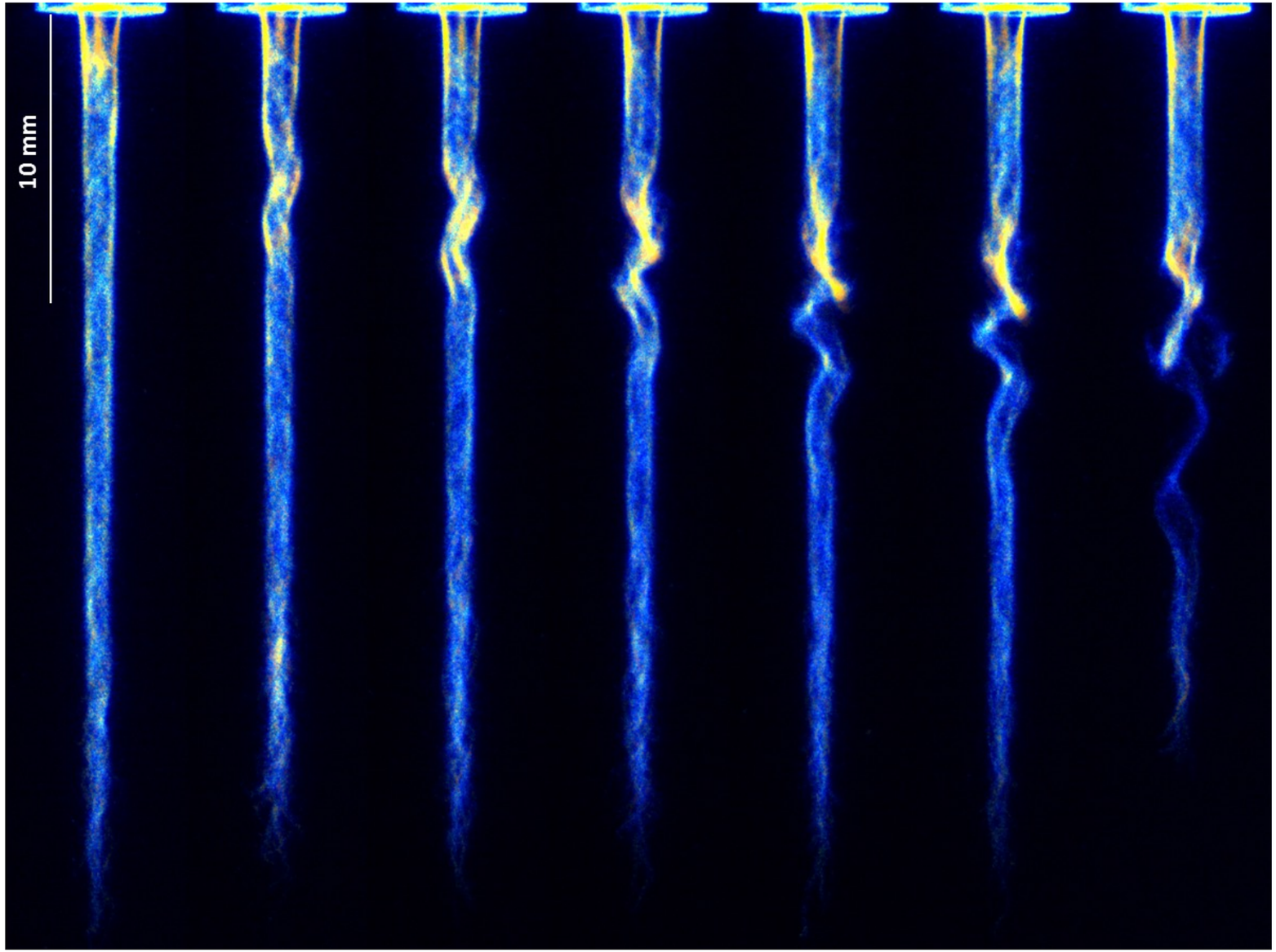

ripple with brightest plasma emission

Breakdown of the argon potential core :

(at least 1 IW stopped in the series of 20)

Very beginning of the flow breakdown :

➡ **1.40 ms**

Prior to the flow breakdown

➡ **ripple** ignition and growth

not visible by using schlieren imaging

Double HV shots

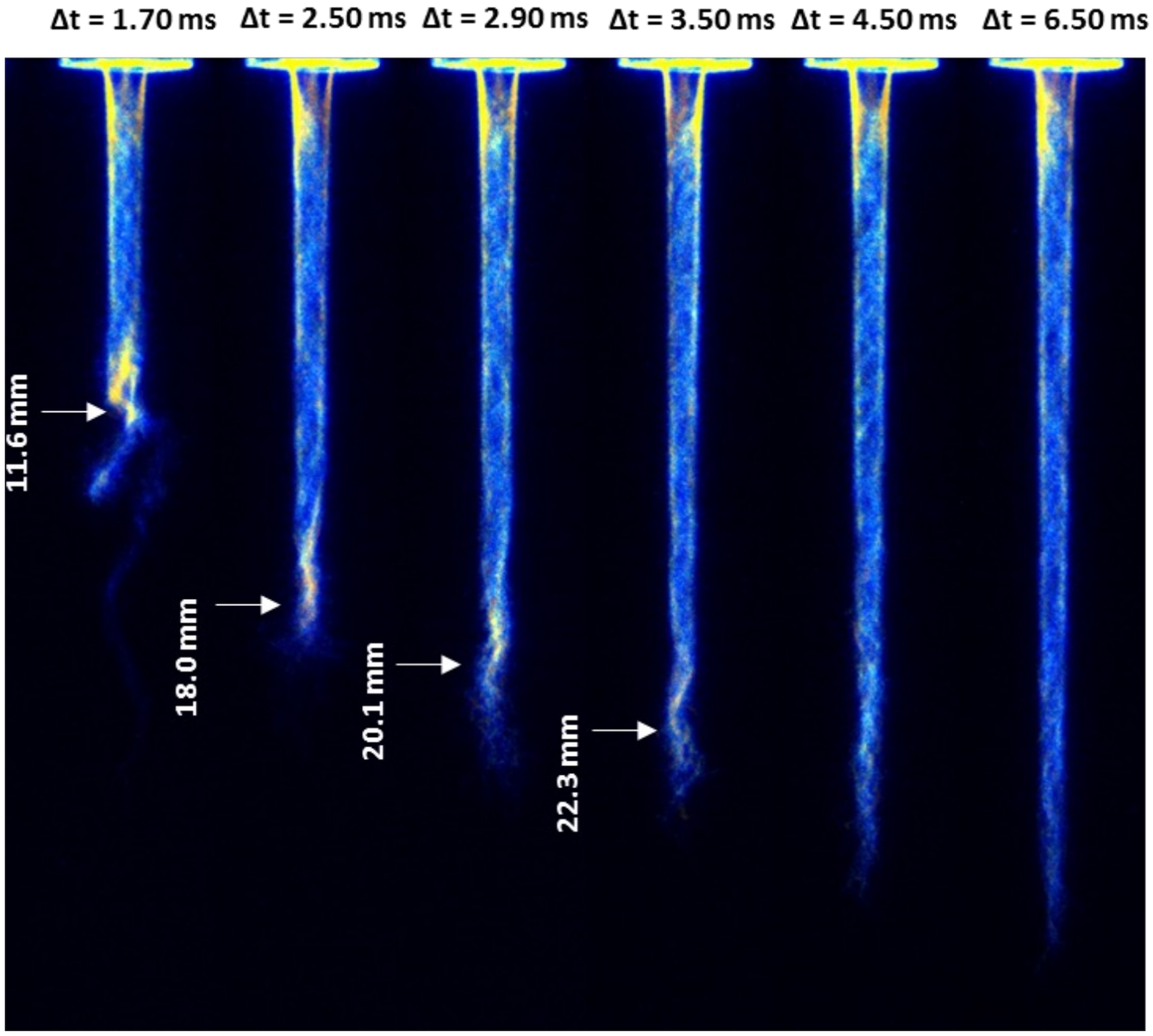

Time to recover the full-length plasma plume

Time to evacuate the flow perturbation

Δt (ms)	Bright plasma plume tip position (mm)	Flow perturbation drift velocity (m/s)
1.70	11.6	12.7
2.50	18.0	8.0
2.90	20.1	5.3
3.50	22.3	3.7

Double HV shots

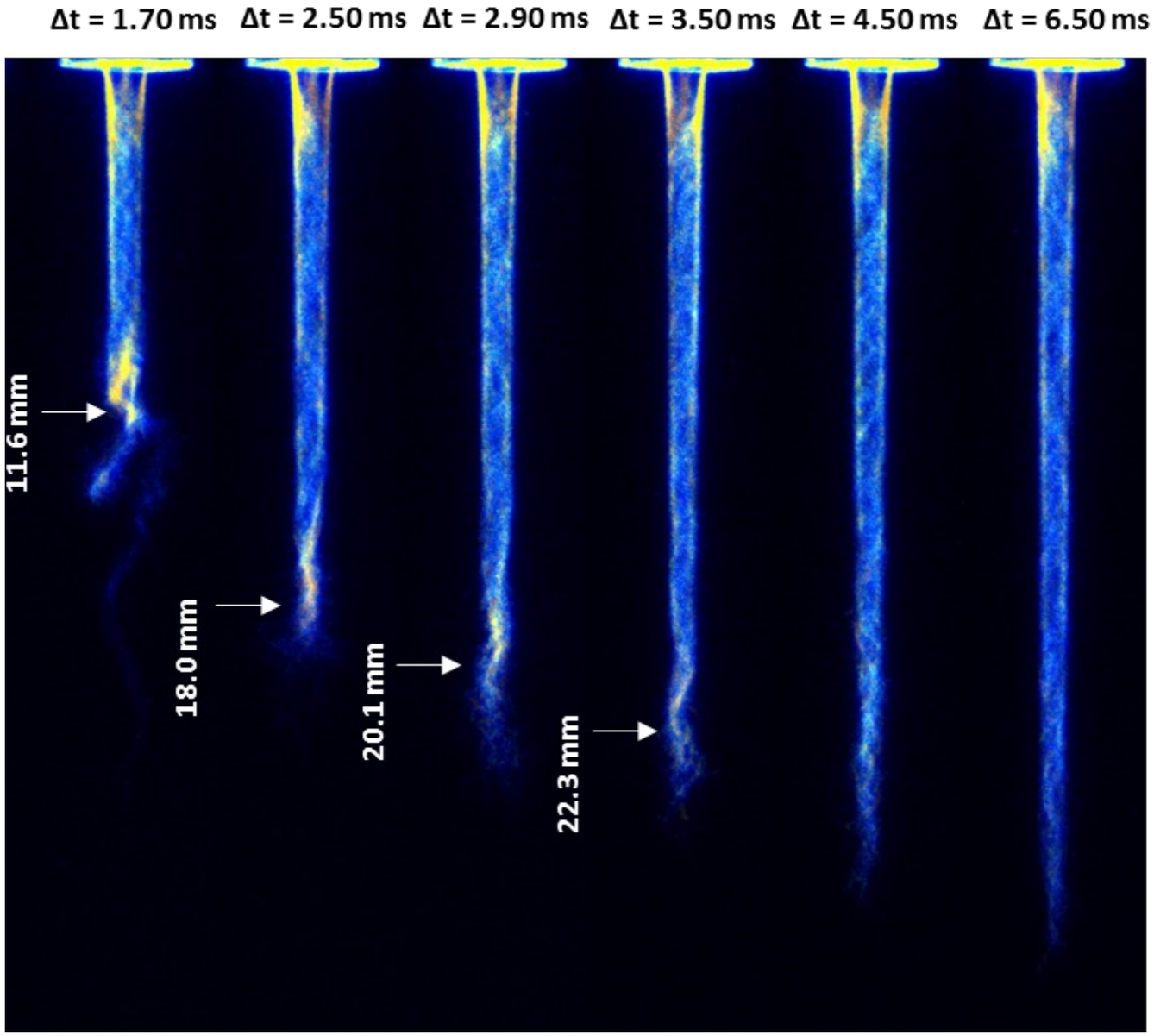

➡ **Perturbation** generated at the inner HV tip

$$\frac{11.6\ mm + 10\ mm}{1.70\ ms} = 12.7\ m/s$$

Mean flow velocity : 11,6 m/s

IW ignition at the inner HV electrode:

➡ **ultra fast heating**

➡ **pressure increase**

The IW propagation has no effect on the flow structure

Single HV shot

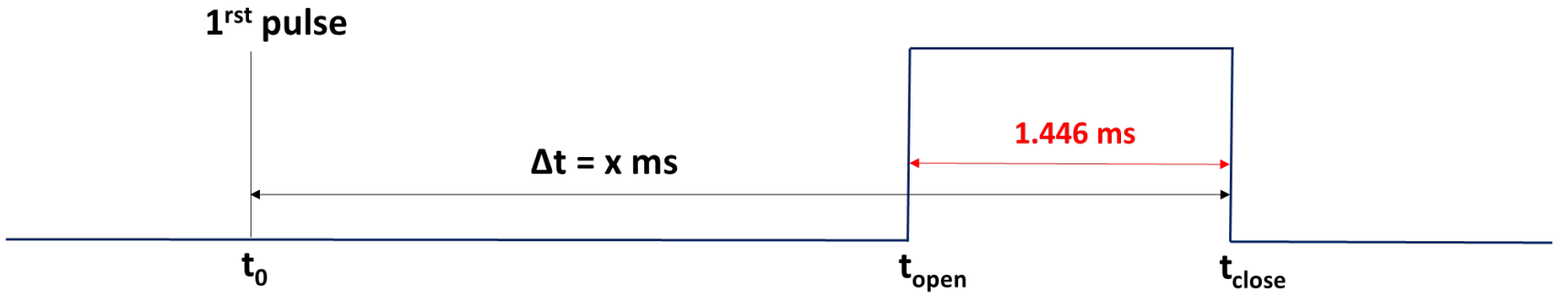

Δt= 0.85 ms

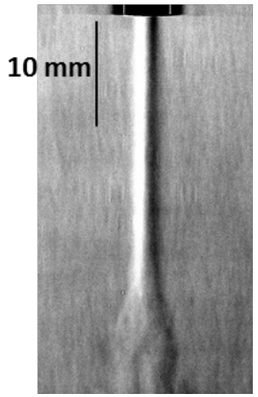

Single HV shot

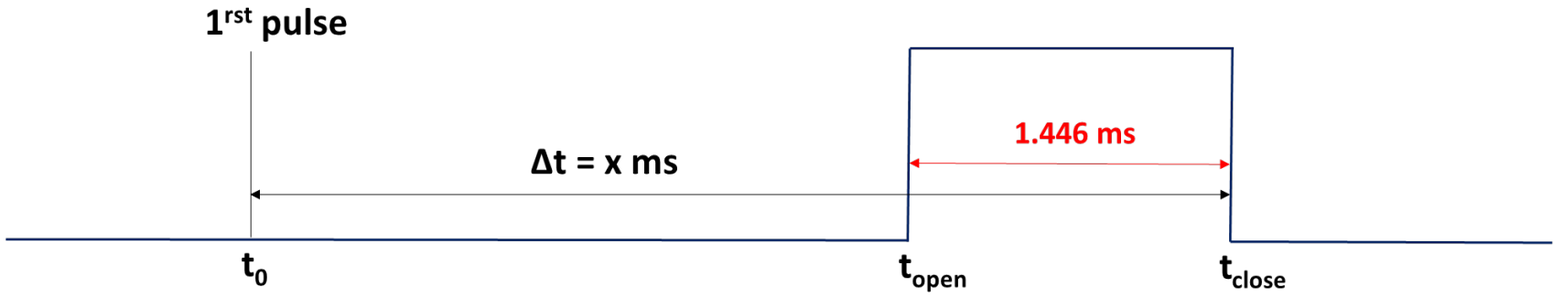

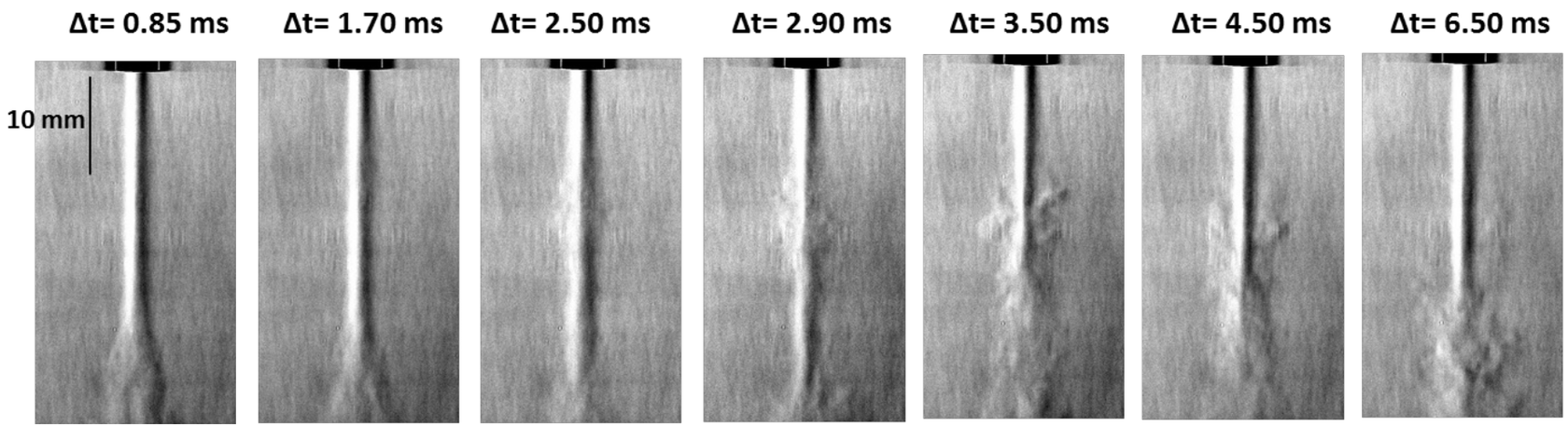

One ionization wave ignition is enough to **break the laminar flow**

Accumulation of perturbations could be expected when multiple HV shots are applied in the kHz regime

- For a 800 sccm flow rate : **6.50 ms to evacuate** the perturbation

Accumulation of perturbations could be expected when multiple HV shots are applied in the kHz regime

Fixed: Δt=3.0 ms

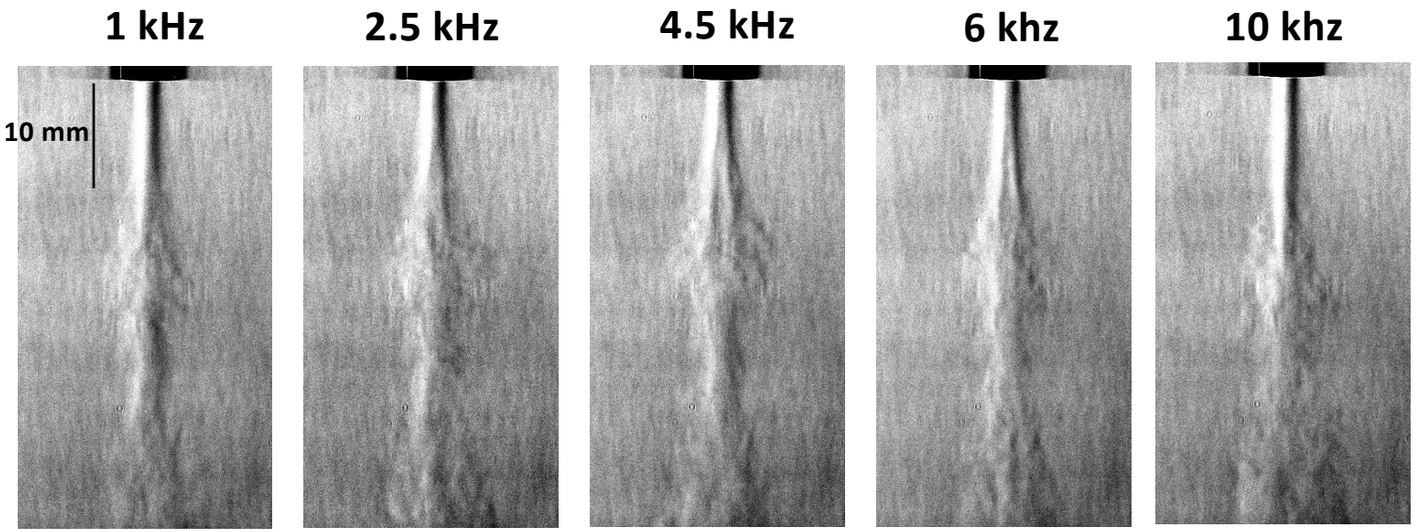

- **From 1 to 4.5 kHz : development of radial splitting of the jet**
- **6 kHz : “closing” of the jet**
- **10 kHz : straight flow**

Multiple HV shots

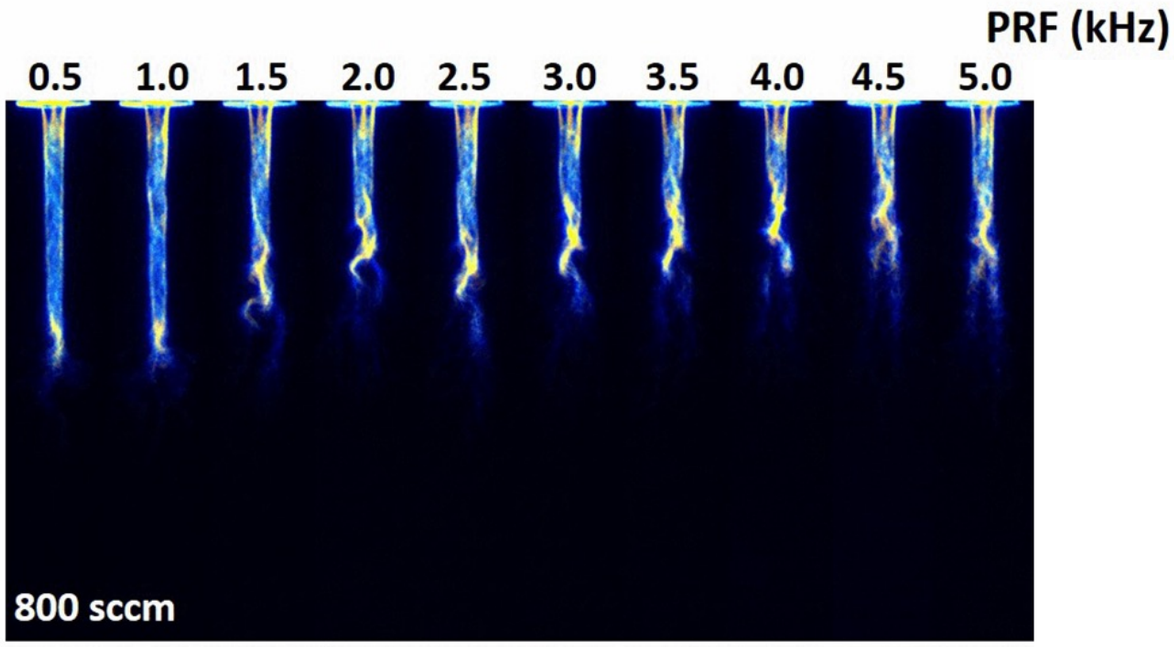

0.5 kHz to 6.0 kHz : ripple alternation in a 3D helical-like arrangement

Multiple HV shots

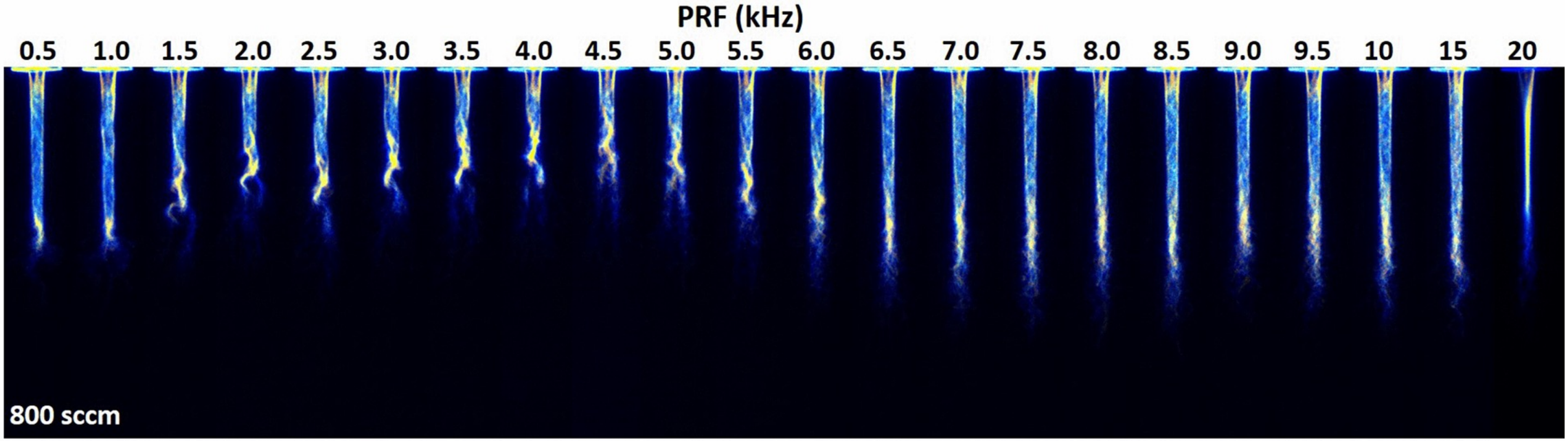

0.5 kHz to 6.0 kHz : ripple alternation in a 3D helical-like arrangement

6 kHz to 20 kHz : Straight plasma plumes

Multiple HV shots

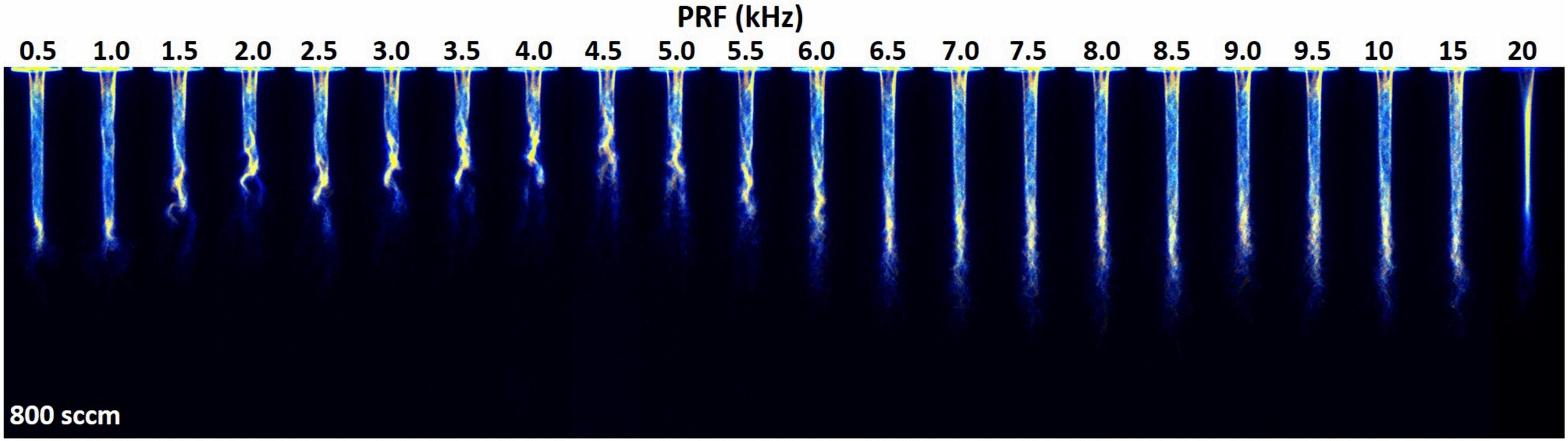

Precise PRF range

- Radial splitting of the jet
- helical-like arrangement of plasma plumes

Beyond transition PRF

- straight flow and plasma plumes

PRF range of 3D helical-like plasma plumes depends on the flow rate

It cannot only be explained by the effect of the accumulation of multiple perturbations inside the gas flow

Mechanism of flow perturbation: Backward-Facing step forced flow

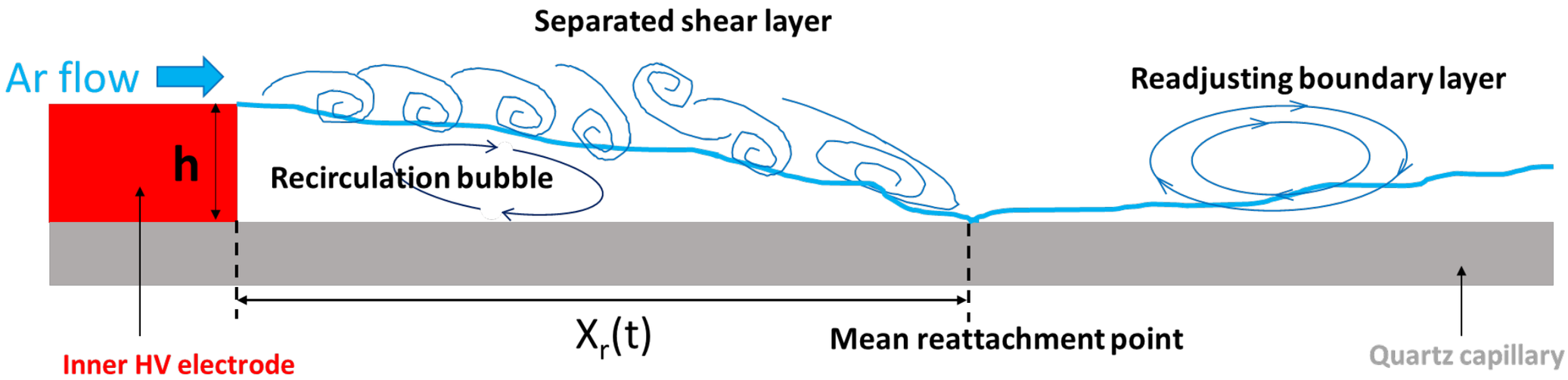

- **Unsteady, absolutely unstable and 3D…**
- **All flow regions are strongly coupled**
- **Large variety of periodic modes and of large-scale coherent vortex structures (driven by Re)**

Extensively studied in fluid mechanics since the 60's (detached-reattached flows)

Mechanism of flow perturbation: Backward-Facing step forced flow

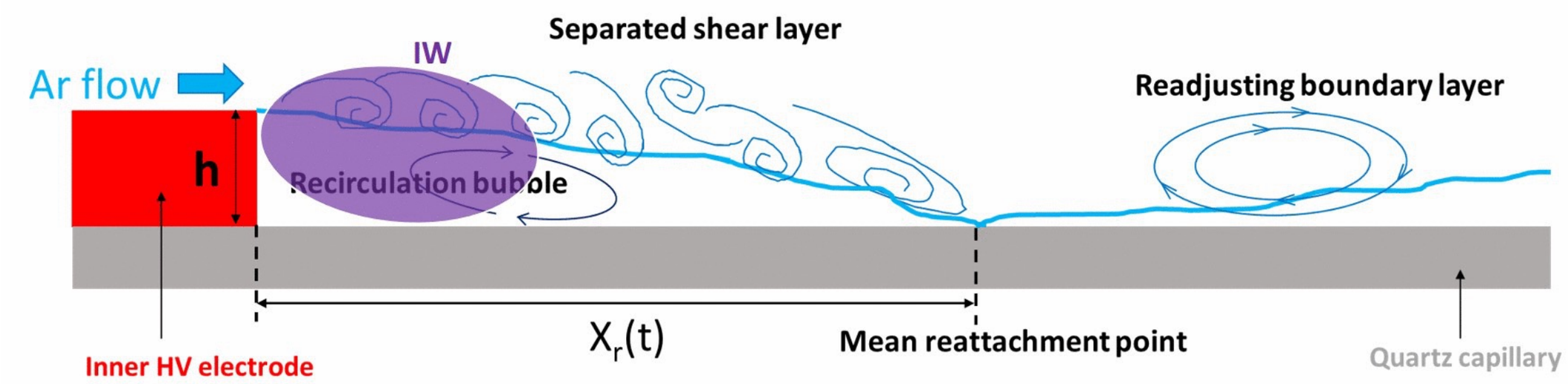

- **Unsteady, absolutely unstable and 3D…**
- **All flow regions are strongly coupled**
- **Large variety of periodic modes and of large-scale coherent vortex structures (driven by Re)**

Extensively studied in fluid mechanics since the 60's (detached-reattached flows)

« beat » between the periodic pressure increase at each IW ignition (driven by PRF) and the flow frequency (driven by Re)

Analog to a forced BFS flow with surface DBD plasma actuator

Conclusion

Study of the **argon flow modification** in a ns **argon CAPPJ**

- Time-resolved schlieren and ICCD imaging
- Application of a single HV pulse (**single HV shot**) to a series of HV pulses at several PRF **(multiple HV shots)**

Only one HV shot is enough to disturb the flow and the plasma plume expansion

With the **double HV shots,** the **second IW** can be used as a **probe**, to **instantly visualize the flow structure** any time after the application of the first HV pulse

multiple HV shots : **Periodic forced flow** through the **repetitive pressure increase** at each IW ignition

Flow control mechanism

It could be easily generalized to other DC pulsed CAPPJ devices, depending on which instabilities modes are accessible to the flow and to which frequencies the flow instability is sensitive

IOP Publishing
Plasma Sources Science and Technology
Plasma Sources Sci. Technol. 30 (2021) 105021 (19pp)
https://doi.org/10.1088/1361-6595/ac2a18

Periodic forced flow in a nanosecond pulsed cold atmospheric pressure argon plasma jet

Thibault Darny, Gérard Bauville, Michel Fleury, Stéphane Pasquiers and João Santos Sousa*

Université Paris-Saclay, CNRS, Laboratoire de Physique des Gaz et des Plasmas, 91405 Orsay, France

E-mail: joao.santos-sousa@universite-paris-saclay.fr

Received 18 June 2021, revised 6 September 2021
Accepted for publication 24 September 2021
Published 25 October 2021

Abstract

This paper is devoted to the study of the argon flow modification in a cold atmospheric pressure plasma jet driven by nanosecond high voltage (HV) pulses, from single to multiple HV shots applications. A schlieren optical bench has been designed in order to visualize the argon flow downstream expansion in quiescent air, for moderate flow rates below 1 standard liter per minute. A coupled approach is used between charge coupled device (CCD) schlieren imaging and intensified CCD (ICCD) plasma plume imaging, both time-resolved. It is shown that the application of only one HV pulse (i.e. single HV shot) is enough to disturb the flow. The disturbed flow exhibits ripple propagation, on a timescale similar to the flow velocity. When operating in double HV shots, the second ionization wave can be used as a probe, to instantly visualize the flow structure any time after the first HV pulse application. For some flow rates, the ripple can increase in amplitude up to the point when it strongly deforms, or even stops, the plasma plume expansion, after which it is entrained by the flow and the plasma plume retrieves its full usual expansion. When a series of HV pulses are applied, the maximal disturbance of the flow is achieved for a certain pulse repetition frequency (PRF), specific of each flow rate. It is associated with ripples alternation in the plasma plume, in a 3D helical-like arrangement. For greater PRF, the ripples progressively vanish, and the flow is clearly less disturbed. Once the ripples have vanished, increasing further the PRF does not change the plasma plume and flow structures. We suggest that the repetitive plasma ignition mechanically forces the flow inside the capillary with consequences on the global flow structure, similarly to a forced backward-facing step flow with actuator.

Thibault Darny *et al.* 2021 *Plasma Sources Sci. Technol.* 30 105021

Surface analysis by plasma assisted mass spectrometry

Kristaq GAZELI, Et-Touhami ES-SEBBAR, Thomas VAZQUEZ, Sara AL-HOMSI, Xavier DAMANY, Gérard BAUVILLE, Michel FLEURY, Pascal JEANNEY, Olivier NEVEU, Blandine BOURNOVILLE, Nicole BLIN-SIMIAND, Stéphane PASQUIERS and João SANTOS SOUSA

Laboratoire de Physique des Gaz et des Plasmas (LPGP)
CNRS & Université Paris-Saclay
Orsay, France

Nanosecond pulsed argon plasma jet reactor

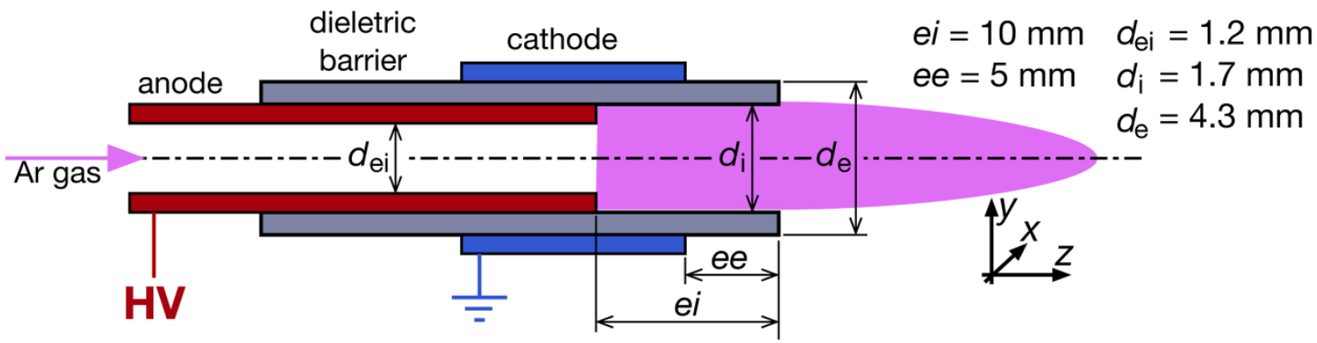

Eur. Phys. J. Appl. Phys. (2016) 75: 24713
Plasma Sources Sci. Technol. 27 (2018) 065003
Plasma Process Polym. 2018; e1800080
J. Appl. Phys. 126, 073302 (2019)
J. Phys. D: Appl. Phys. 53 (2020) 475202

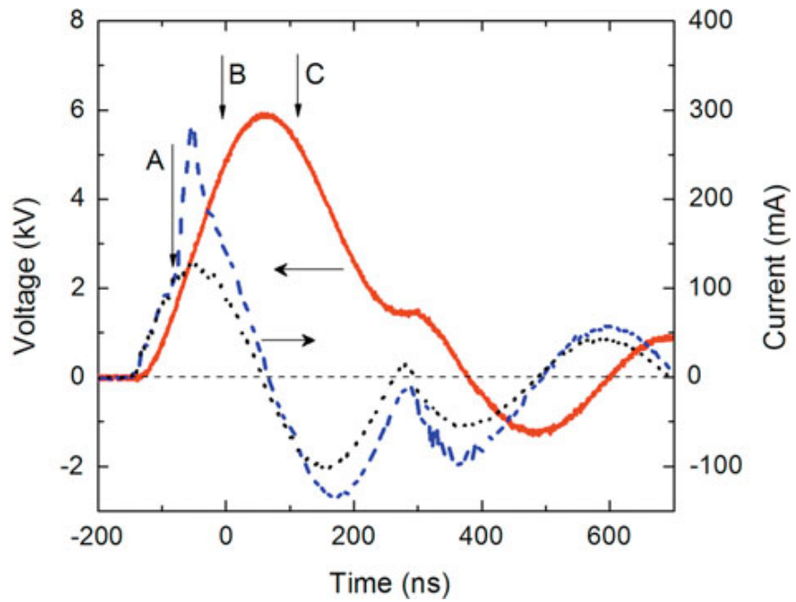

Fig. 1. Time evolution of the current (total current: blue dashed line, displacement current: black dotted line) and the voltage (red solid line) for an applied HV pulse of 6.0 kV at 20 kHz. Arrows A, B, C, please refer to the text.

Nanosecond pulsed argon plasma jet: fast imaging

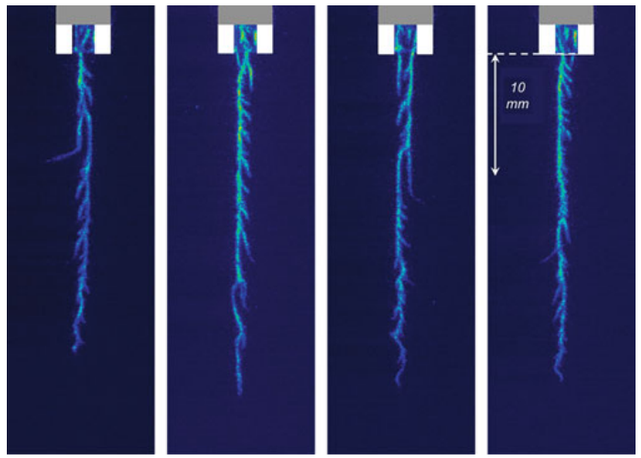

Fig. 2. Plasma emission captured by ICCD camera for an exposure time of 200 ns and for single HV pulses. Experimental parameters: 6 kV, 20 kHz, 0.7 L/min NTP, free argon jet.

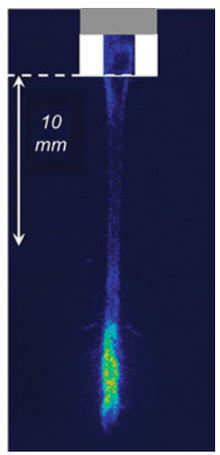

Fig. 3. Plasma emission captured by ICCD camera for an exposure time of 20 ns, and accumulated over 10 successive HV pulses. Same experimental parameters as those of Figure 2.

Eur. Phys. J. Appl. Phys. (2016) 75: 24713

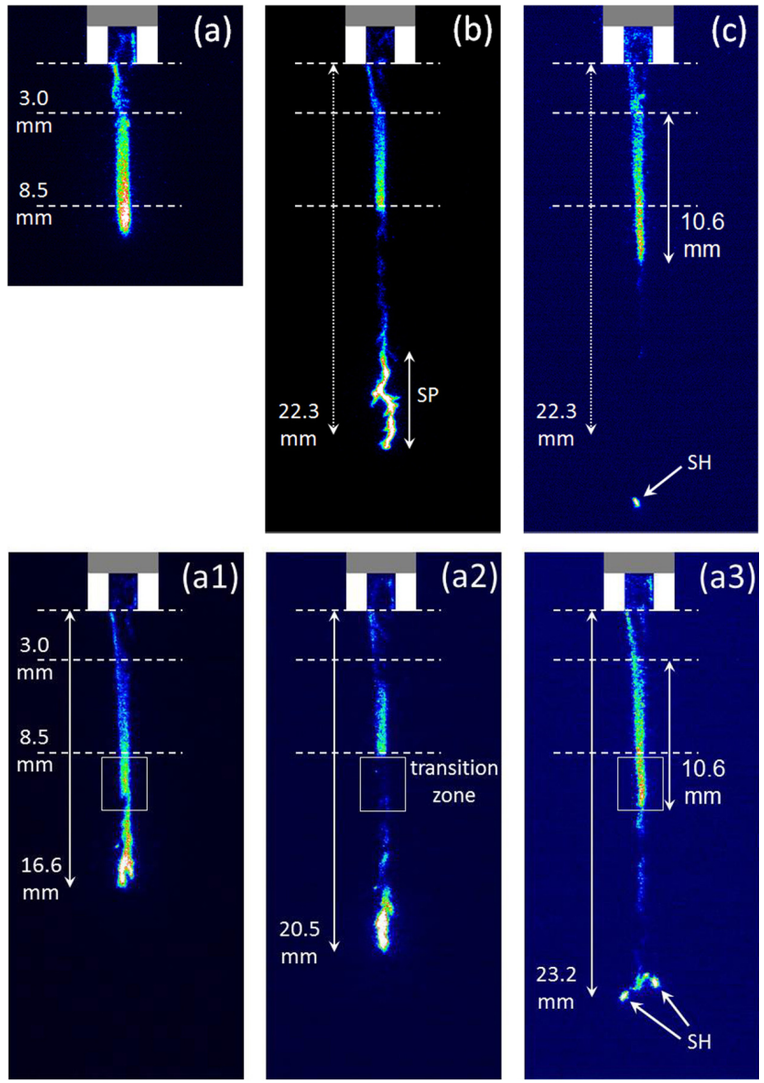

FIG. 3. Light emission from the DBD-MPJ captured by an ICCD camera, over only one single HV pulse. The applied voltage is 6.0 kV and the Ar flow rate is 750 sccm. Images (a), (a1), (a2), and (a3) were acquired 93 ns, 123 ns, 153 ns, and 173 ns after the peak of the discharge current, respectively, for an exposure time of 5 ns. A transition zone is highlighted with a rectangular box in (a1)–(a3). In (a3), two distinct streamer's heads (SH) are identified. In (b) (20 ns of exposure time and 153 ns after the peak current), SP denotes the spatial distribution of the streamers propagation over 20 ns. In (c) (10 ns of exposure time and 221 ns after the peak current), the position of one streamer's head (SH) at maximum propagation is pointed out.

J. Appl. Phys. 126, 073302 (2019)

Nanosecond pulsed argon plasma jet: fast imaging

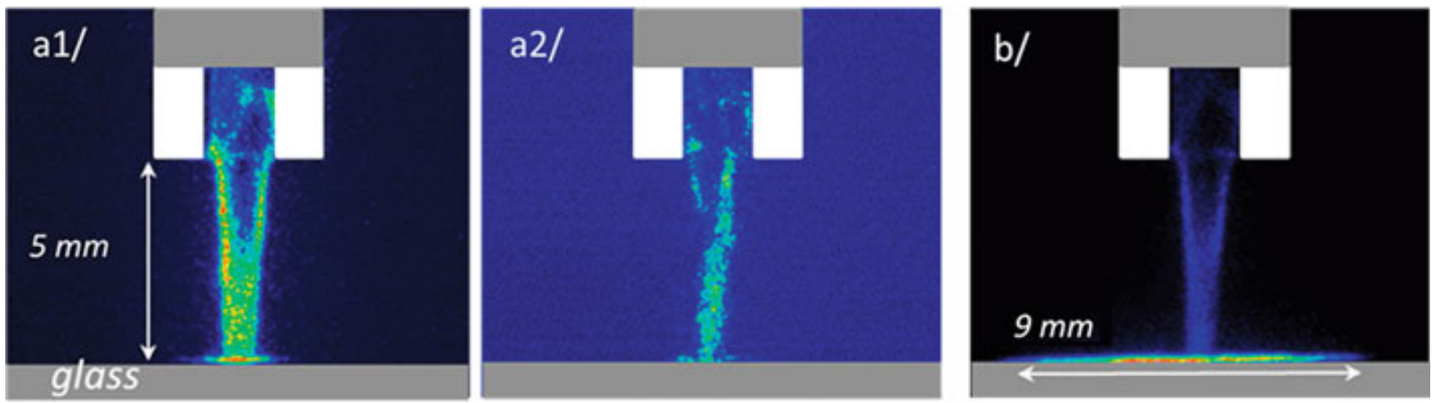

Fig. 4. Plasma emission captured by ICCD camera for an exposure time of 20 ns. Distance from nozzle to plate: 5 mm. Cases a1/, a2/, and b/: please refer to the text. Same experimental parameters as those of Figure 2.

Eur. Phys. J. Appl. Phys. (2016) 75: 24713

Nanosecond pulsed argon plasma jet: fast imaging

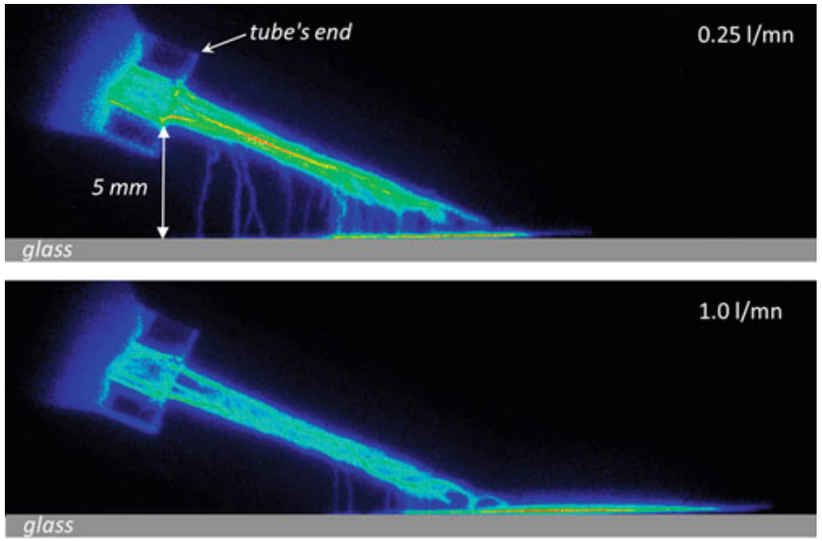

Fig. 5. Plasma emission captured by ICCD camera for an exposure time of 250 ns and accumulated over 10 successive HV pulses. Distance from nozzle to plate: 5 mm. Angle between the glass surface and the tube axis: 25°. Discharge parameters: 6 kV, 20 kHz. The argon flow rate values are given in the pictures.

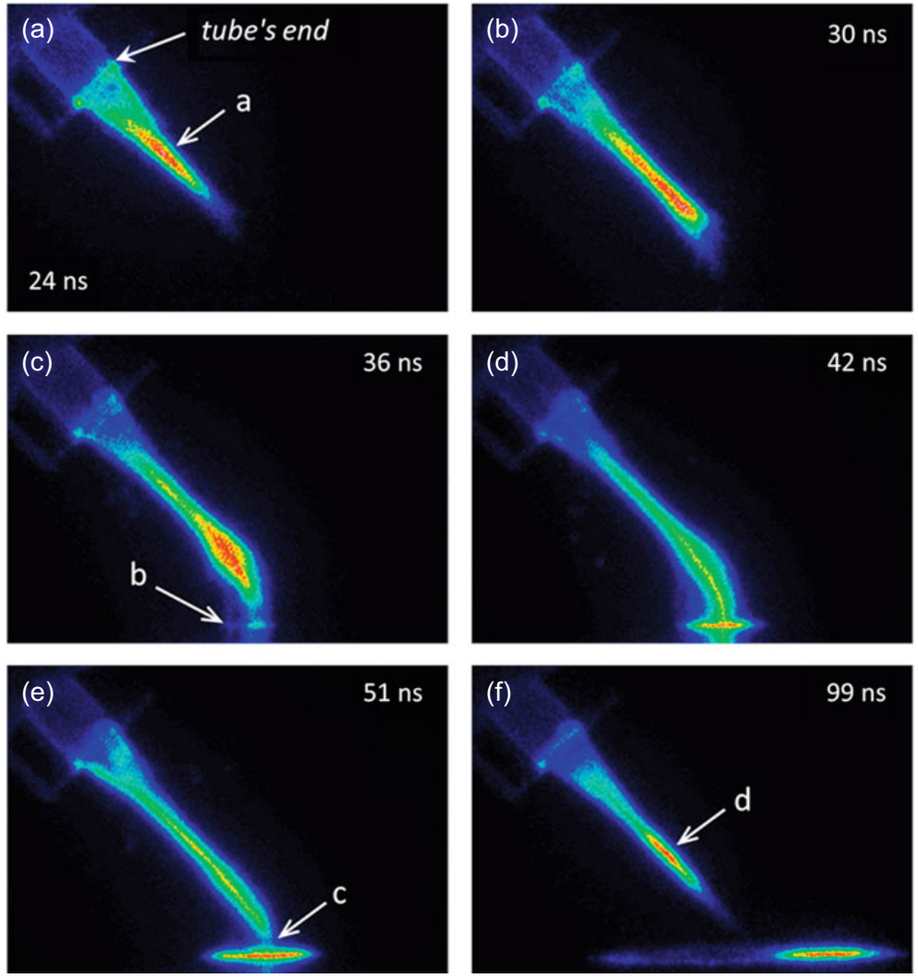

Fig. 6. Plasma emission captured by ICCD camera for an exposure time of 3 ns and accumulated over 100 successive HV pulses. Distance from nozzle to plate: 5.5 mm. Angle between the glass surface and the tube axis: 45°. Discharge parameters: 6 kV, 20 kHz. Argon flow rate: 0.25 L/min NTP. Time scale and arrows denoted "a", "b", "c", "d": please refer to text.

Eur. Phys. J. Appl. Phys. (2016) 75: 24713

Nanosecond pulsed argon plasma jet: desorption

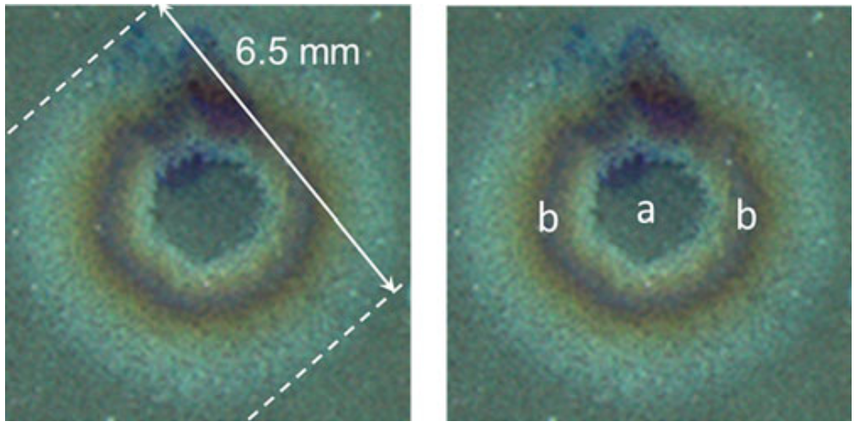

Fig. 7. The bibenzyl deposit on a glass surface after a perpendicular argon plasma jet treatment, showing the partial removal of the film. Discharge parameters: 6 kV, 20 kHz. Discharge running time: 10 s. Gas flow rate: 0.25 L/min NTP. Distance from nozzle to plate: 8 mm. Axis of the argon jet perpendicular to the plate. Areas denoted "a" and "b": see text.

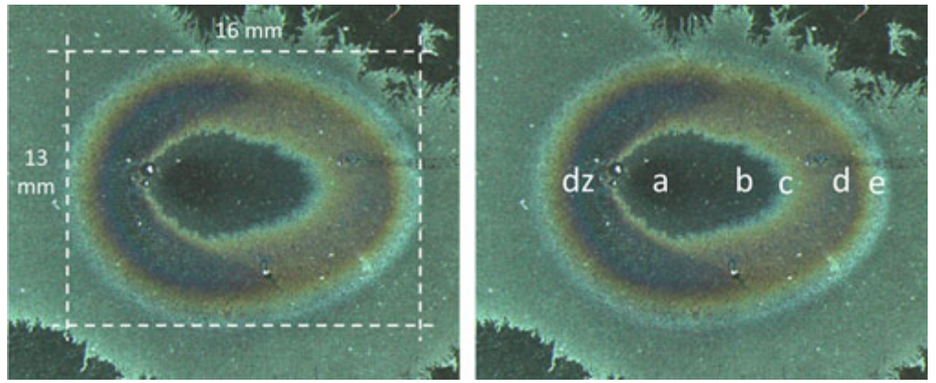

Fig. 8. The bibenzyl deposit on a glass surface after a non-perpendicular argon plasma jet treatment, showing the partial removal of the film. Discharge parameters: 6 kV, 20 kHz. Discharge running time: 60 s. Gas flow rate: 0.25 L/min NTP. Distance from nozzle to plate: 5 mm. Angle between the argon jet and the plate: 45°. Areas denoted "a", "b", "c", "d", "e", and "dz": see text.

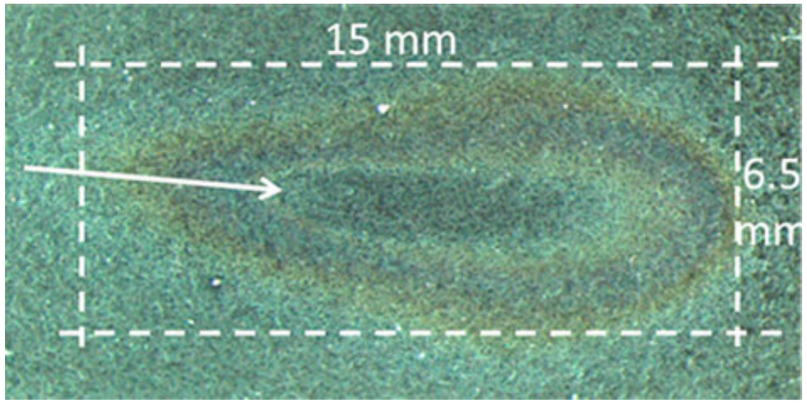

Fig. 9. The bibenzyl deposit on a glass surface after a non-perpendicular argon plasma jet treatment, showing the partial removal of the film. Discharge parameters: 6 kV, 20 kHz. Discharge running time: 30 s. Gas flow rate: 0.5 L/min NTP. Distance from nozzle to plate: 5 mm. Angle between the jet and the plate: 25°. The arrow shows the direction of propagation of the argon jet.

Eur. Phys. J. Appl. Phys. (2016) 75: 24713

Nanosecond pulsed argon plasma jet: setup

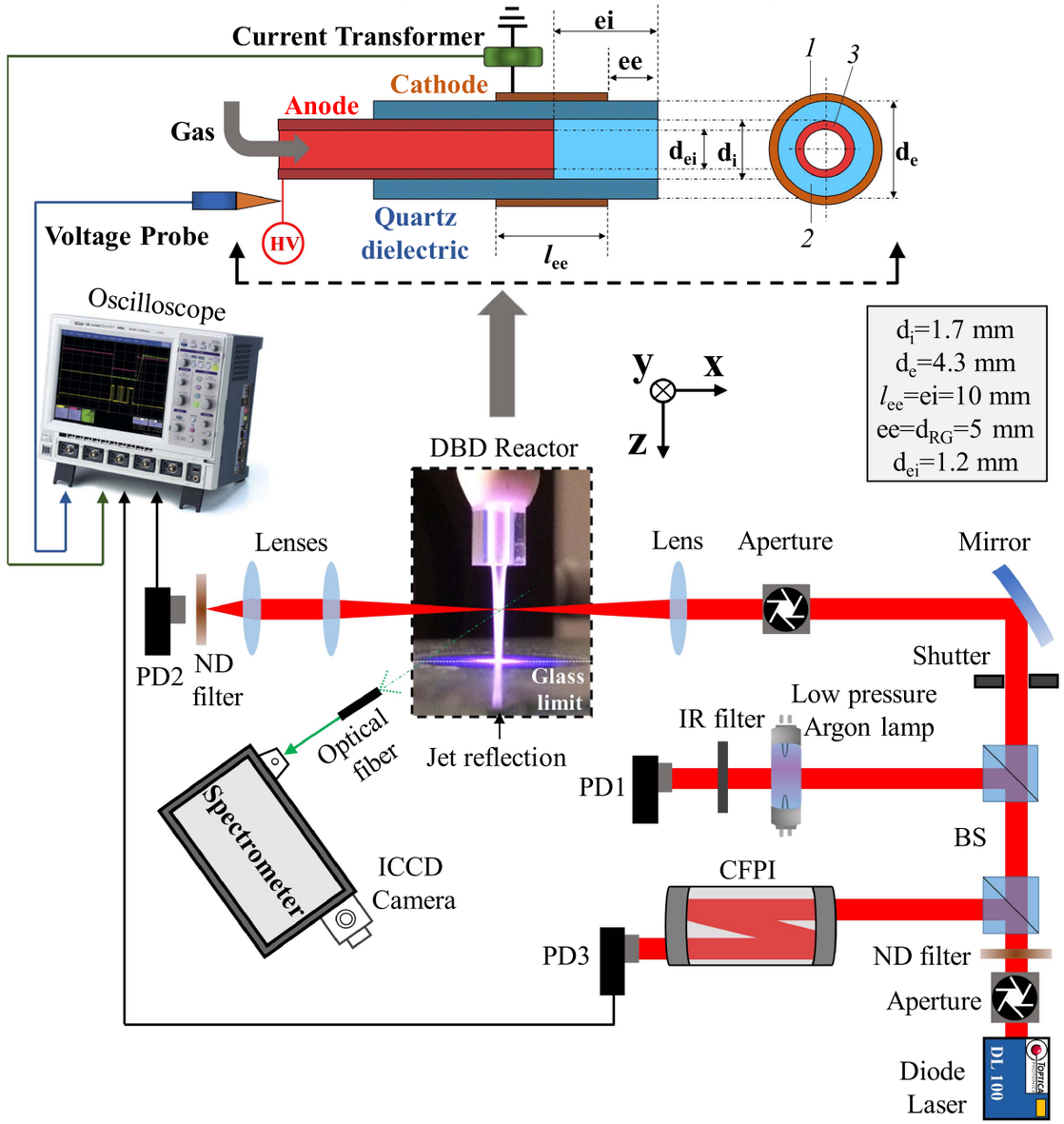

Figure 1. Upper part: side section and front view of the DBD reactor used for the production of the streamers impacting the glass surface. Lower part: experimental TDLAS setup used in this work for the measurement of the argon metastables absolute densities. IR filter: infrared filter, PD (1, 2, 3): photodiode, ND filter: neutral density filter, CFPI: confocal Fabry–Perot interferometer, BS: beam splitter, dRG: distance between the reactor's nozzle and the glass plate.

Plasma Sources Sci. Technol. 27 (2018) 065003

Nanosecond pulsed argon plasma jet: setup

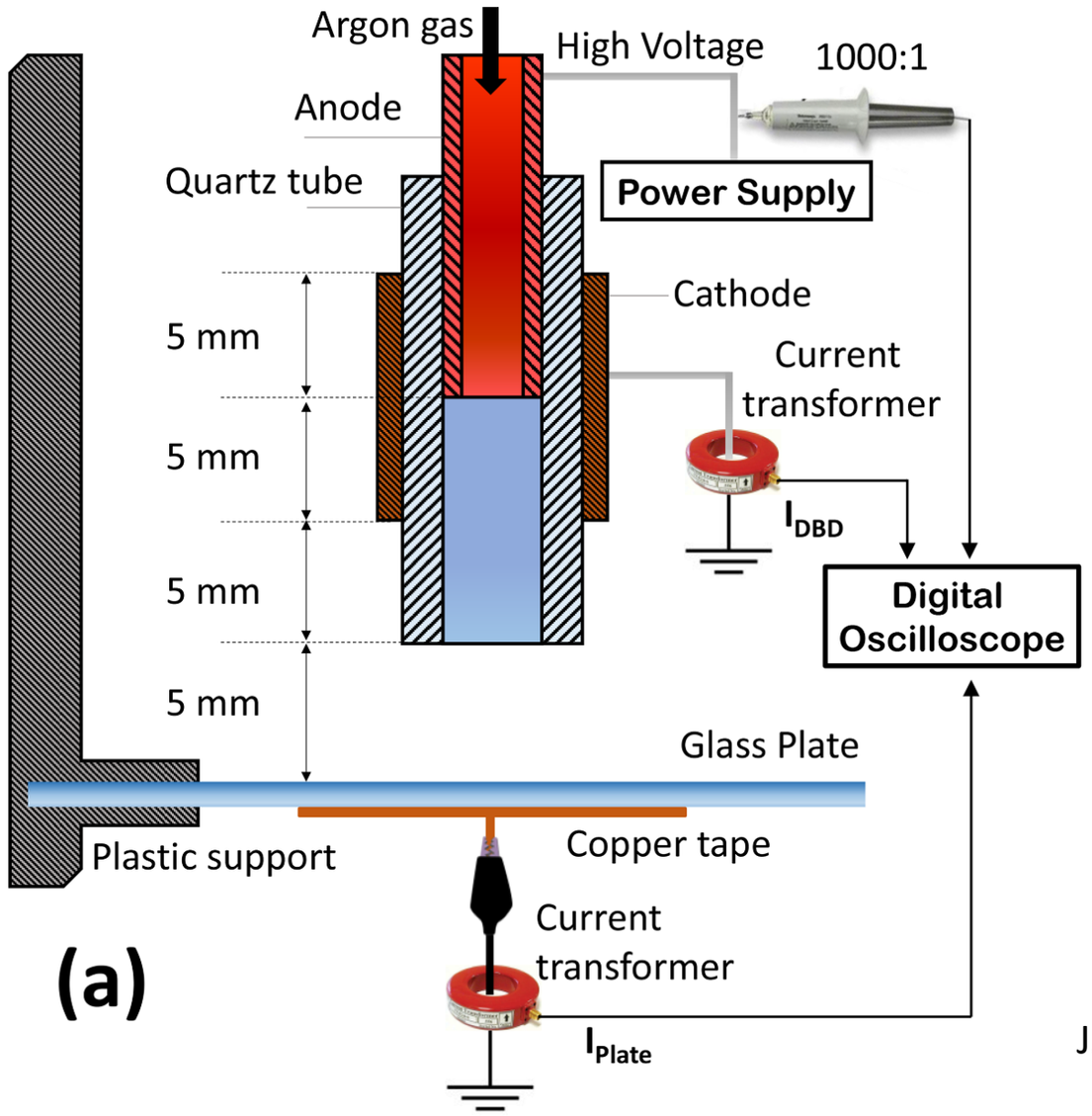

J. Phys. D: Appl. Phys. 53 (2020) 475202

Nanosecond pulsed argon plasma jet: electrical measurements

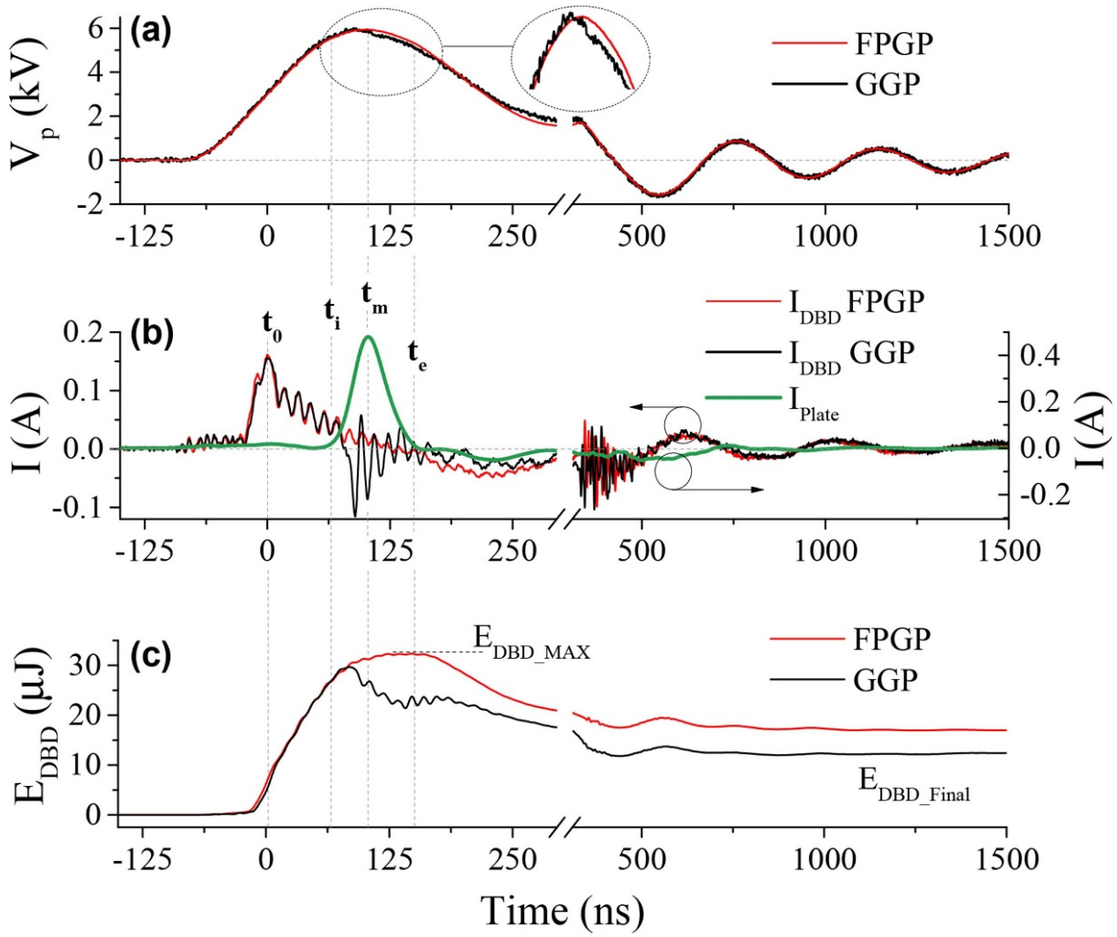

J. Phys. D: Appl. Phys. 53 (2020) 475202

Figure 2. (a) Applied voltage (V_p), (b) conduction current of the DBD (I_{DBD}), and total current recorded through the wire connecting the tape glued under the glass plate and the circuit's ground when the plate is grounded (I_{Plate}—green), and (c) energy of the DBD (E_{DBD}) over a voltage pulse, for the cases of a floating-potential glass plate (FPGP, red) and a grounded (GGP, black) glass plates.

Nanosecond pulsed argon plasma jet: imaging

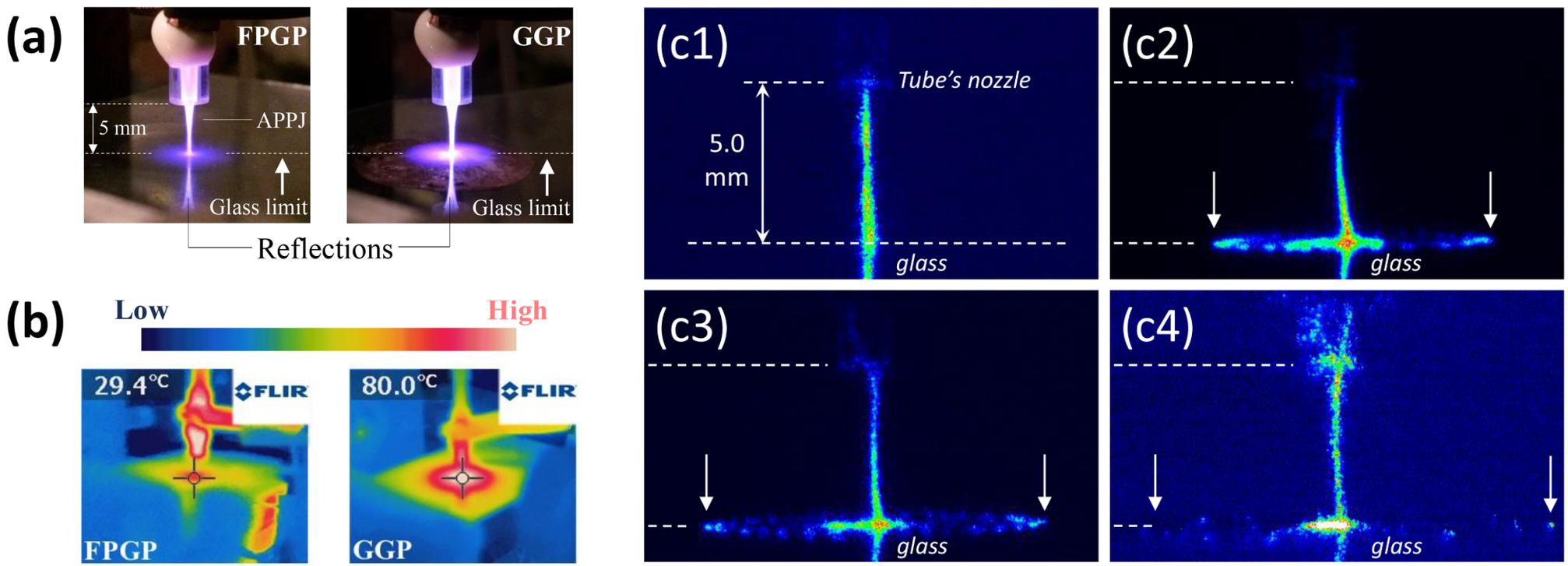

diameter of the area covered by the SIW (luminous 'disk' in (a)): up to 13 mm
almost 10x the tube diameter

J. Phys. D: Appl. Phys. 53 (2020) 475202

Nanosecond pulsed argon plasma jet: Ar*

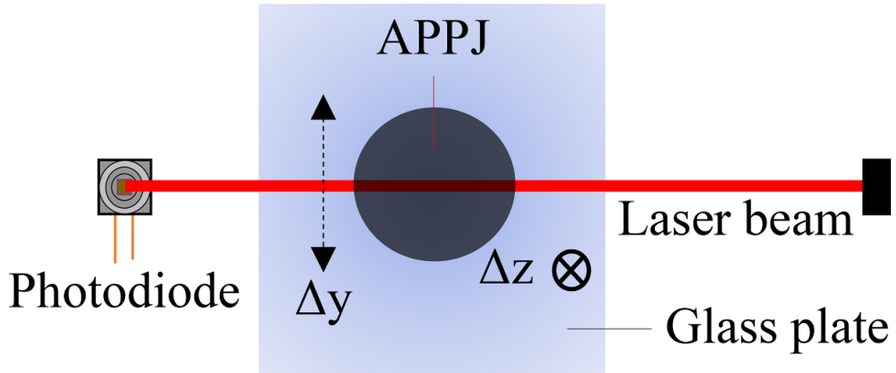

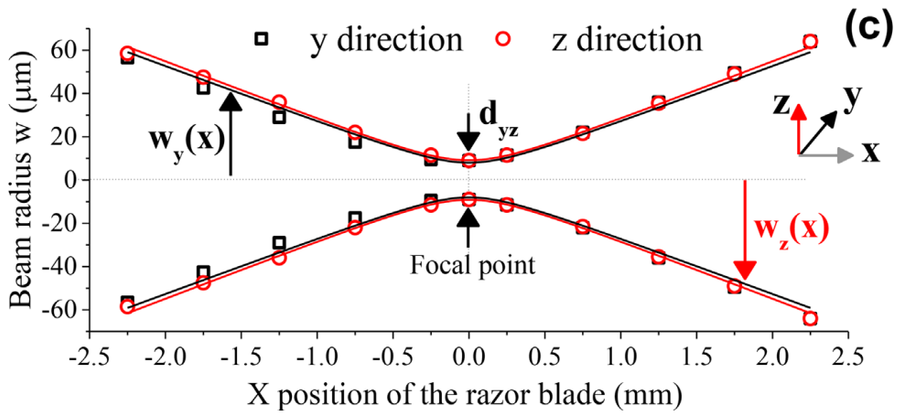

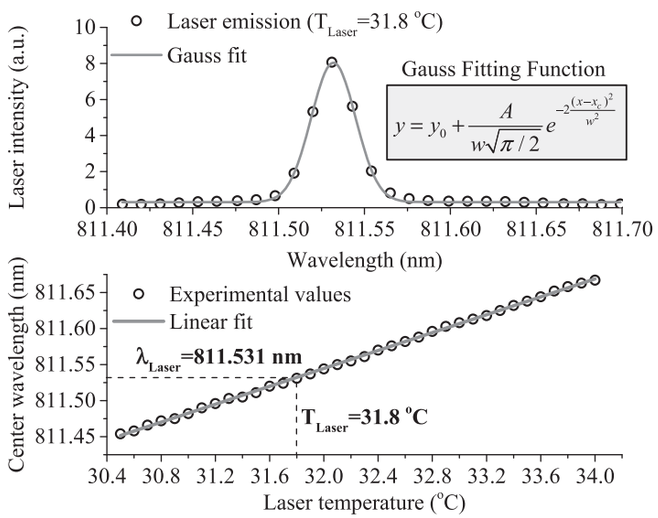

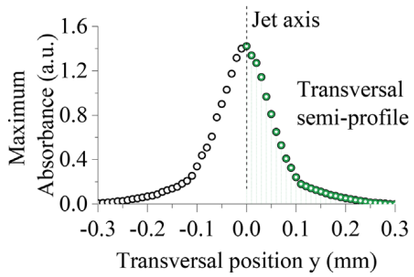

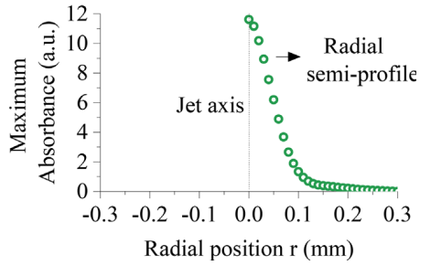

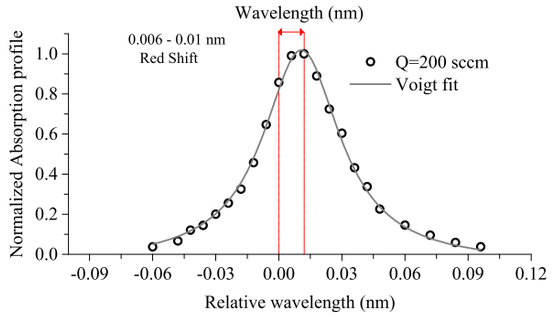

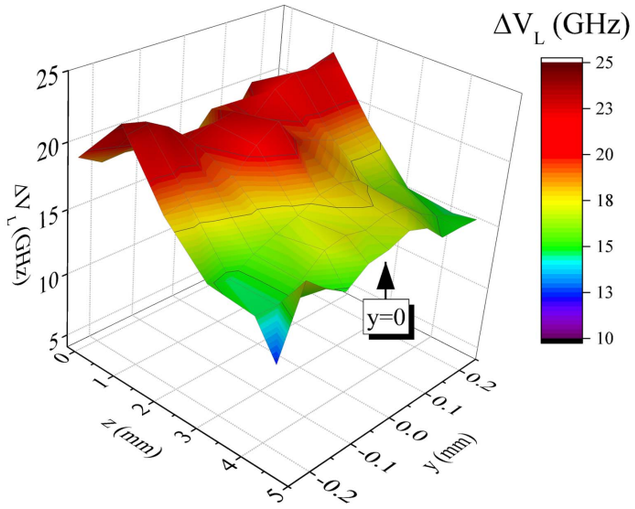

Plasma Sources Sci. Technol. 27 (2018) 065003

Plasma Process Polym. 2018; e1800080

Nanosecond pulsed argon plasma jet: Ar*

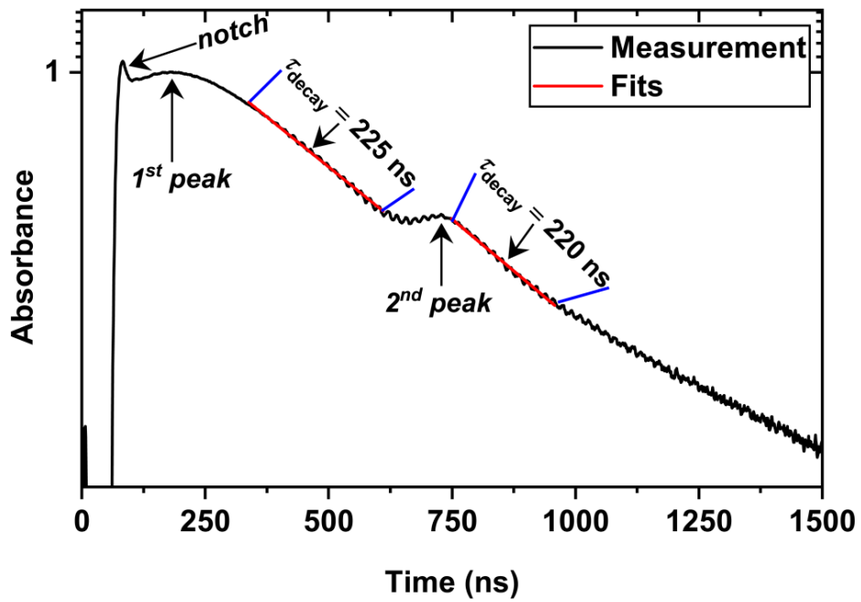

FIG. 8. Typical decay fits of the measured absorbance (at z = 3.35 mm and y = 0 mm) using Eq. (3), for the determination of the Ar($1s_5$) effective lifetimes after the first and the second absorption peaks. The solid blue lines define the limits of the fitting intervals. Ar flow rate = 750 sccm and applied voltage = 6.0 kV.

Plasma Sources Sci. Technol. 27 (2018) 065003
J. Appl. Phys. 126, 073302 (2019)

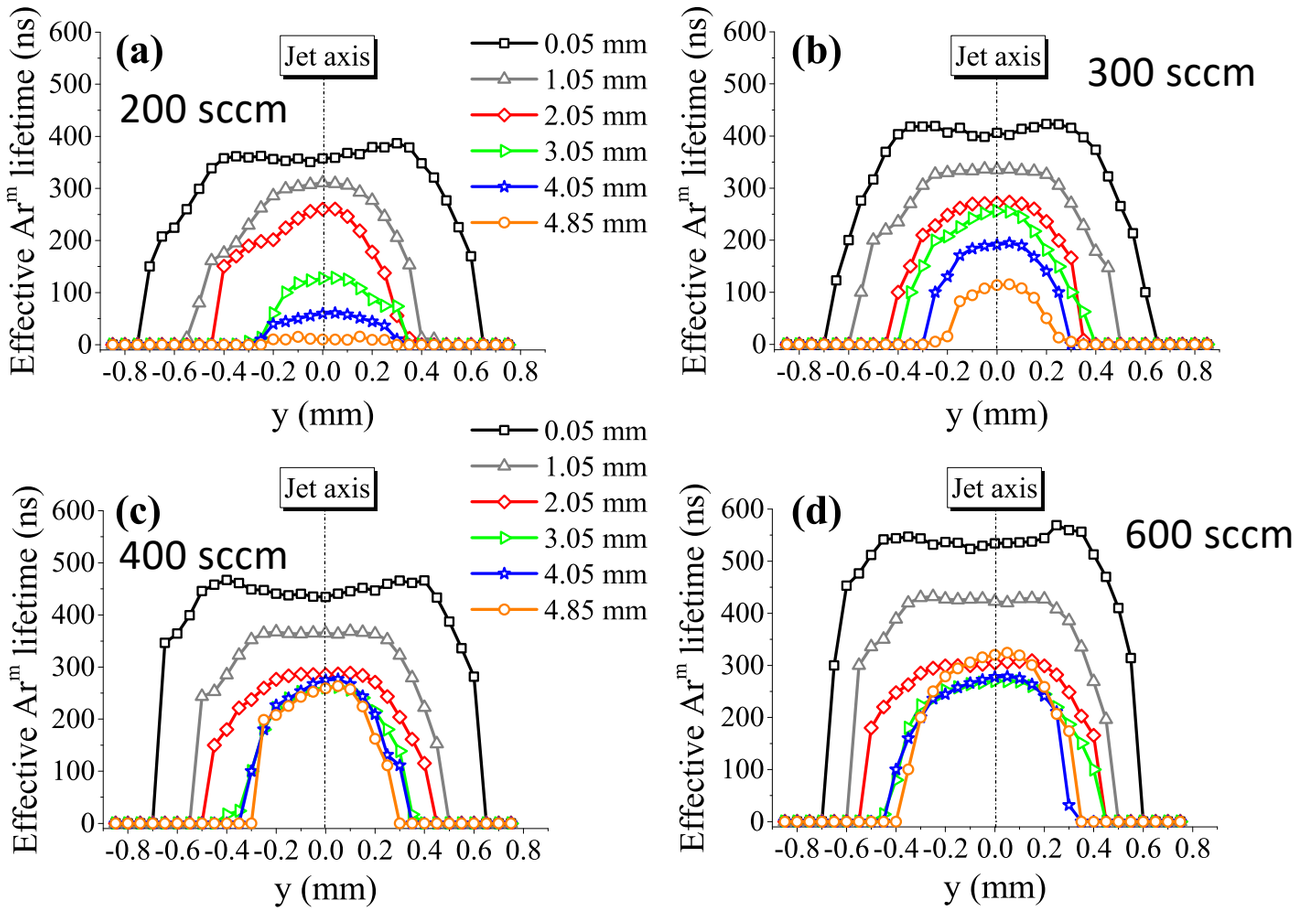

Figure 14. Ar($1s_5$) effective lifetime (τ_e) as a function of selected values of the axial and transversal coordinates at (a) 200, (b) 300, (c) 400 and (d) 600 sccm. Each τ_e value is obtained from a density curve averaged over 10 000 signals in the oscilloscope. $V_p = 6$ kV, $f = 20$ kHz.

Nanosecond pulsed argon plasma jet: Ar*

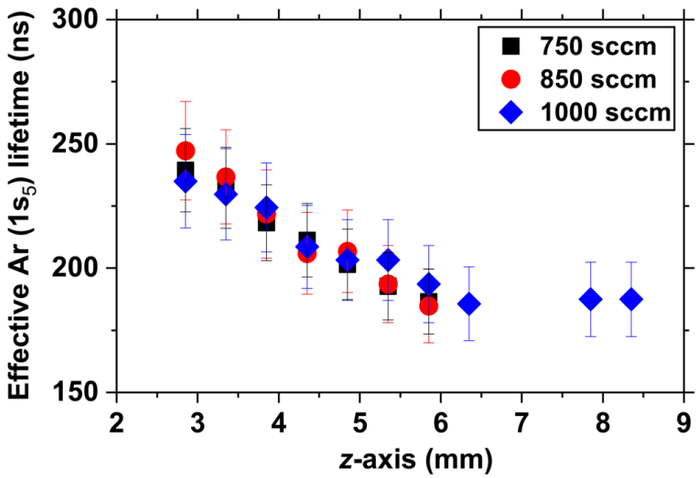

FIG. 10. Longitudinal (z-axis) profile of the effective Ar($1s_5$) lifetimes averaged over 4 HV pulses, obtained from the fits of the decay of the absorbance after the first absorption peak, for three Ar flow rates: 750, 850, and 1000 sccm. The measurements were performed at the center of the MPJ (y = 0) for an applied voltage of 5.2 kV.

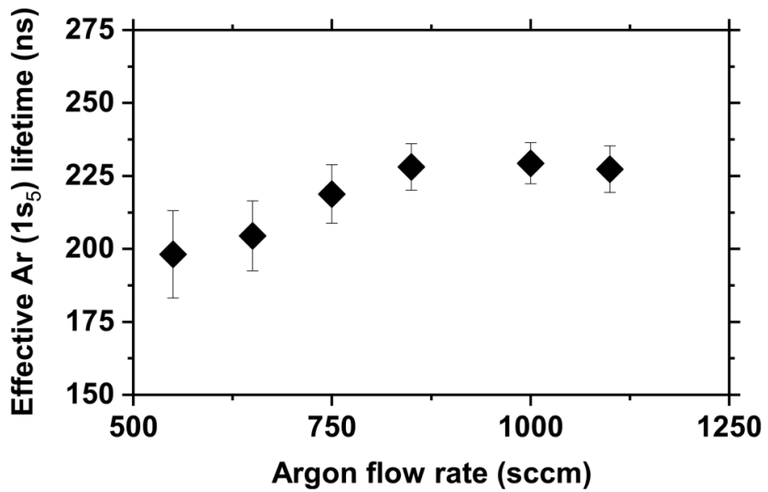

FIG. 11. Effect of the Ar flow rate on the effective Ar($1s_5$) lifetimes averaged over 4 HV pulses, obtained from the fits of the decay of the absorbance after the first absorption peak, at the center of the MPJ (y = 0) and at z = 3.85 mm downstream from the nozzle of the capillary tube. Applied voltage = 5.2 kV.

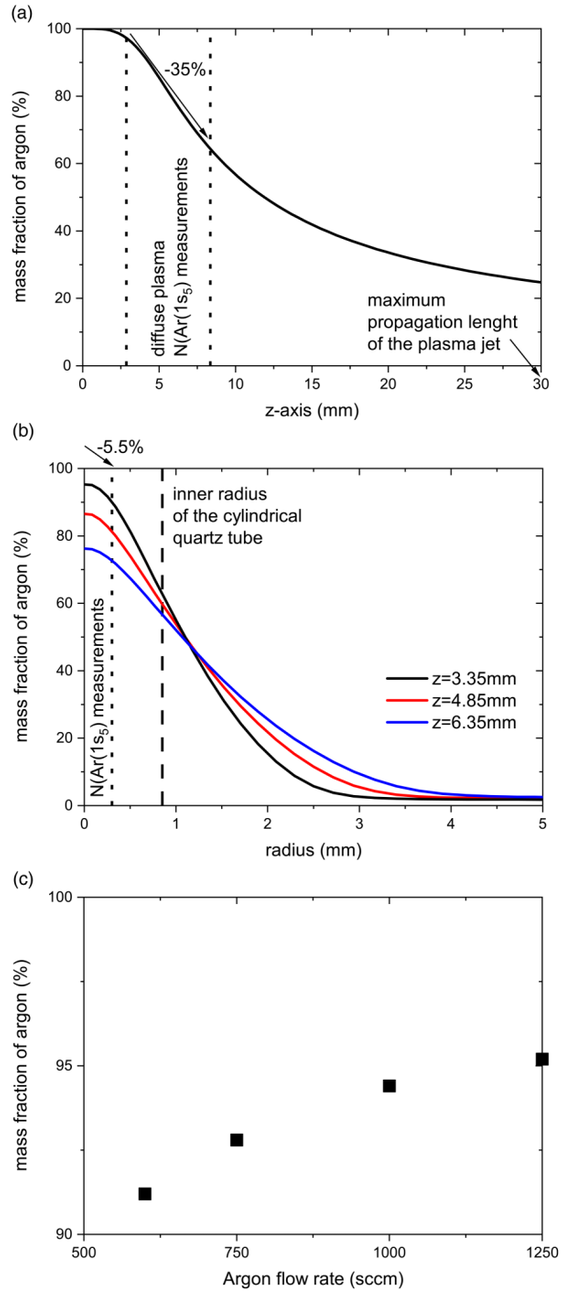

FIG. 4. Mass fraction of argon calculated by a k-ε turbulence multispecies fluid dynamics model (a) along the longitudinal axis (z-axis) at the center of the argon jet (i.e., y = 0) for an argon gas flow rate of 750 sccm, (b) along the radial position at three longitudinal positions downstream from the nozzle of the capillary tube (z = 3.35, 4.85, and 6.35 mm) for an argon gas flow rate of 750 sccm, and (c) as a function of the argon gas flow rate at the center of the jet (i.e., y = 0) and at z = 3.85 mm downstream from the nozzle of the capillary tube.

J. Appl. Phys. 126, 073302 (2019)

Thanks to A. Michau (LSPM, CNRS, Univ. Paris 13, France)!

Nanosecond pulsed argon plasma jet: Ar*

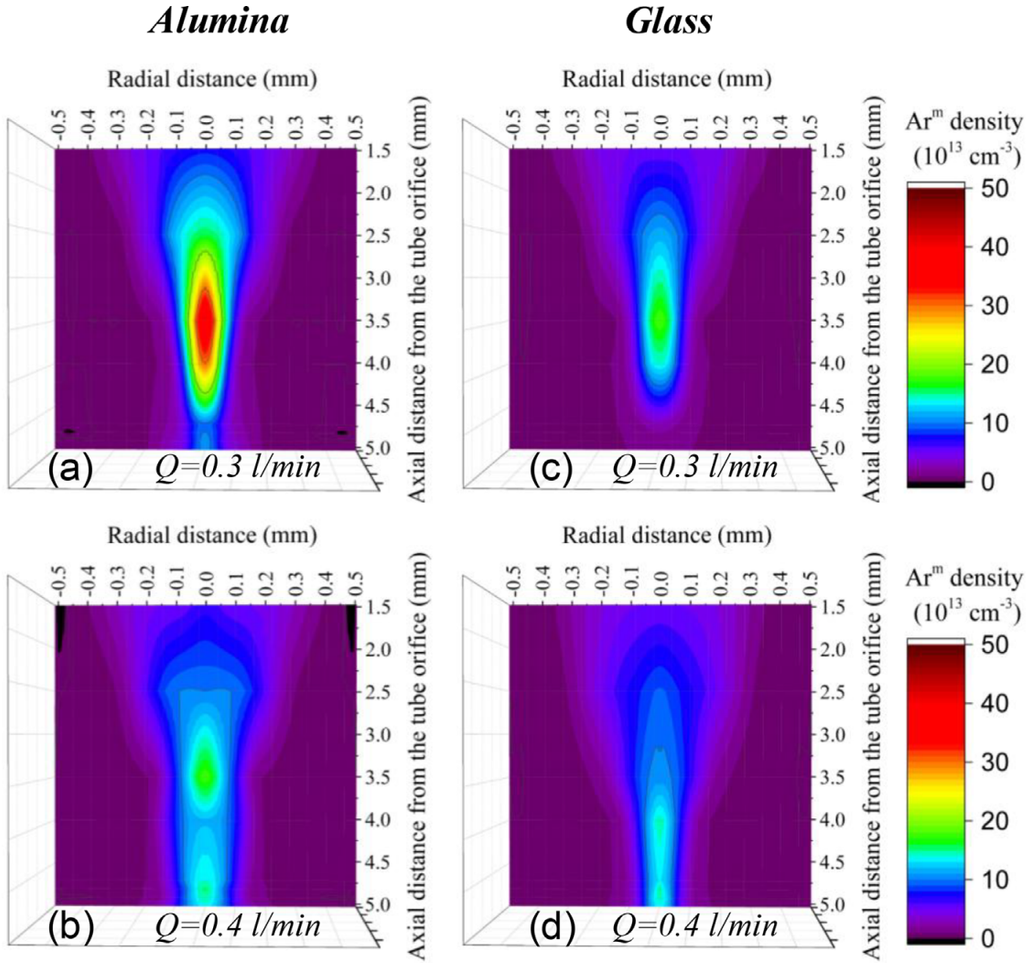

FIGURE 6 2D mappings in the z–r plane of the $N^{r}_{Ar^m}$ for both targets and gas flow rates. The axis of propagation (center of the jet) is at $r = 0$ mm. $V_p = 6$ kV, $f = 20$ kHz

Plasma Process Polym. 2018; e1800080

Nanosecond pulsed argon plasma jet: Ar*

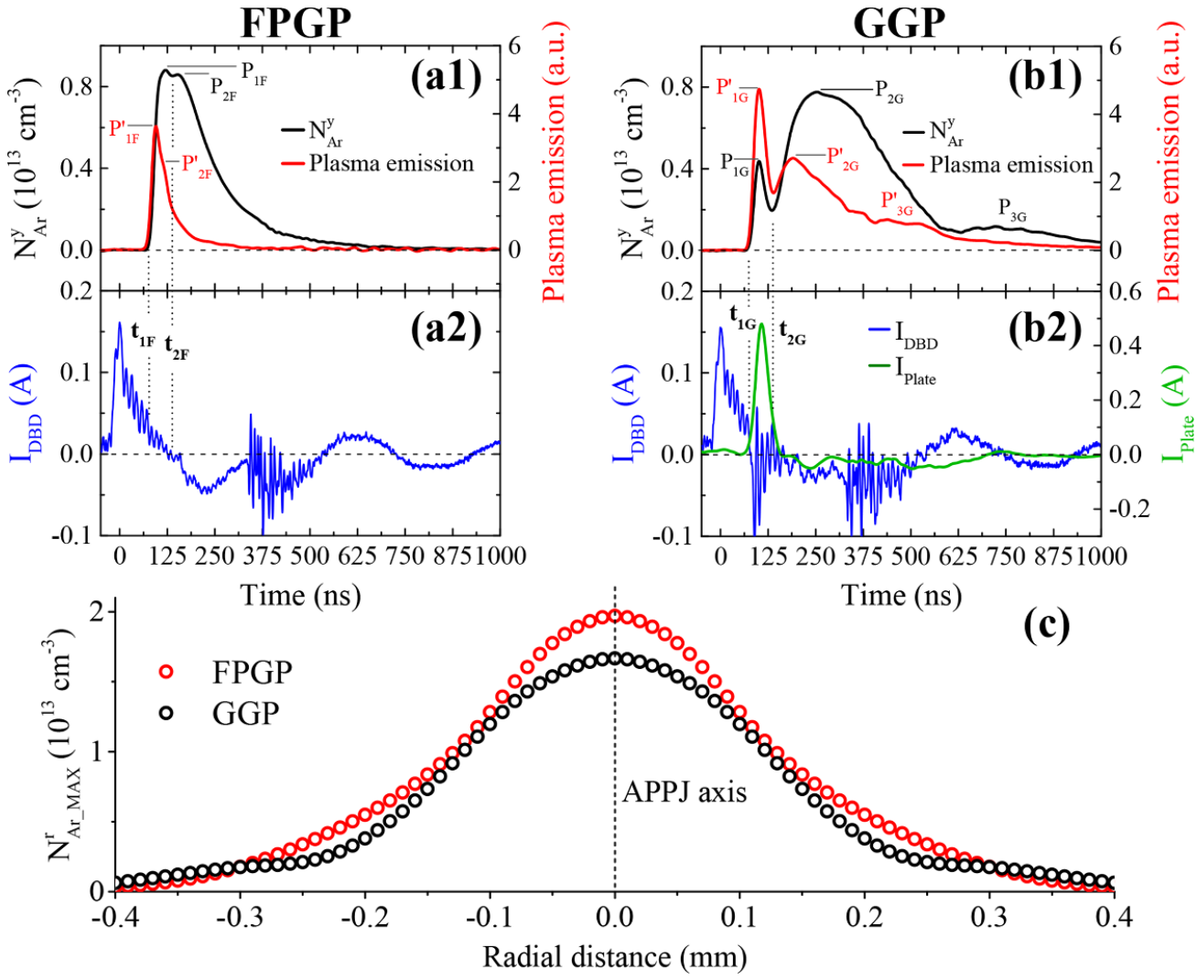

Figure 4. Temporal evolution of the line-of-sight averaged density of Ar($1s_5$) (N^y_{Ar}, black) and the wavelength-integrated (320–1000 nm) plasma emission (red) at z = 4.8 mm and y = 0, I_{DBD} (blue) and I_{Plate} (green) in the case of a floating-potential glass plate (FPGP, (a1) and (a2)) and a grounded glass plate (GGP, (b1) and (b2)). (c) Ar($1s_5$) maximum density symmetric radial profiles ($N_{Ar}{}^r{}_{\_MAX}$) at z = 4.8 mm. All sub-figures show average waveforms obtained from 1000 signals in the oscilloscope.

J. Phys. D: Appl. Phys. 53 (2020) 475202

Nanosecond pulsed argon plasma jet: OES

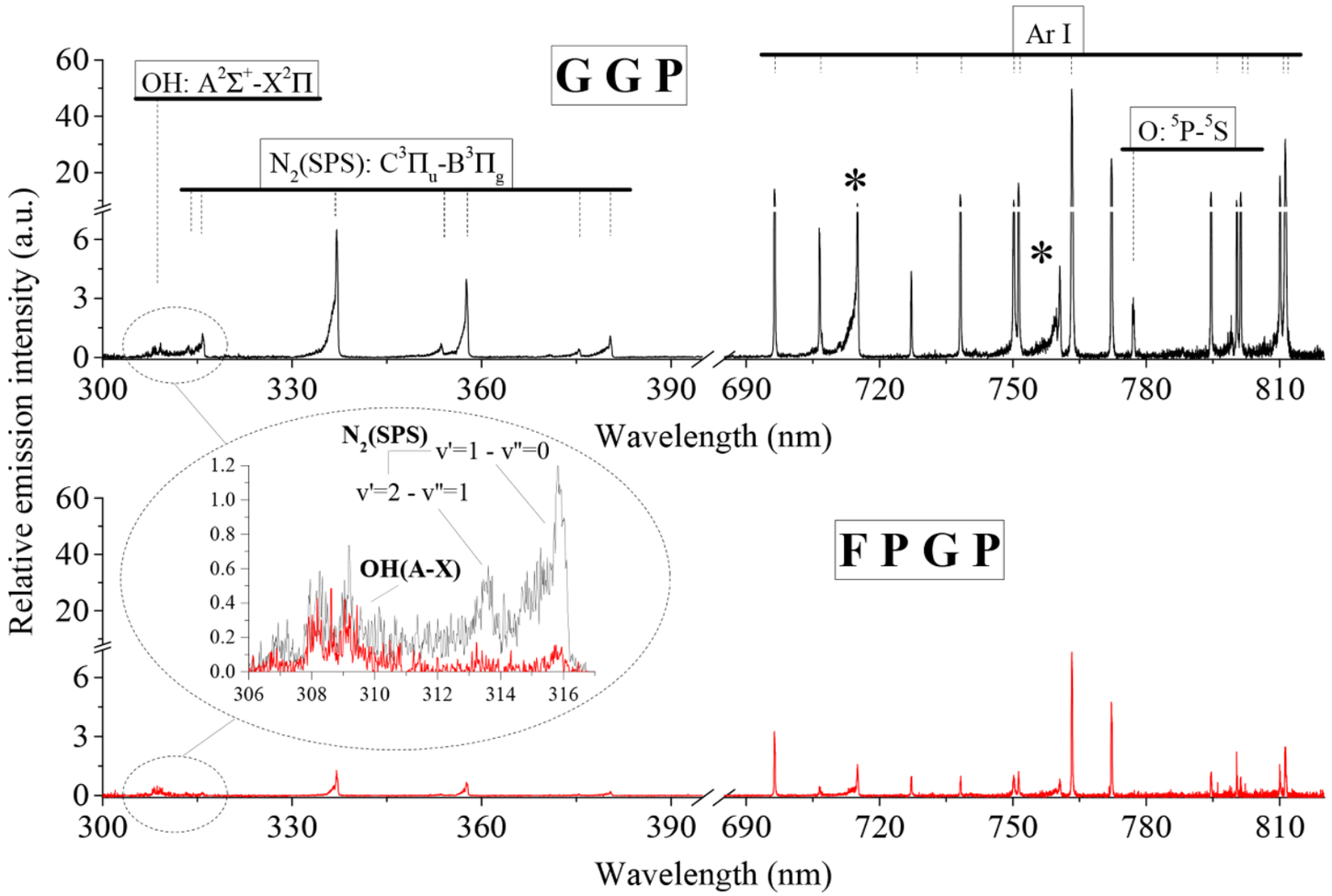

J. Phys. D: Appl. Phys. 53 (2020) 475202

Figure 5. Emission spectrum (UV–NIR) of the APPJ in the case of a grounded glass plate (GGP, black, upper frame) and a floating-potential glass plate (FPGP, red, lower frame). The inset is a zoom in the spectral region 306–316 nm. The asterisks denote second-order spectra of the N_2(SPS).

Nanosecond pulsed argon plasma jet: temperatures

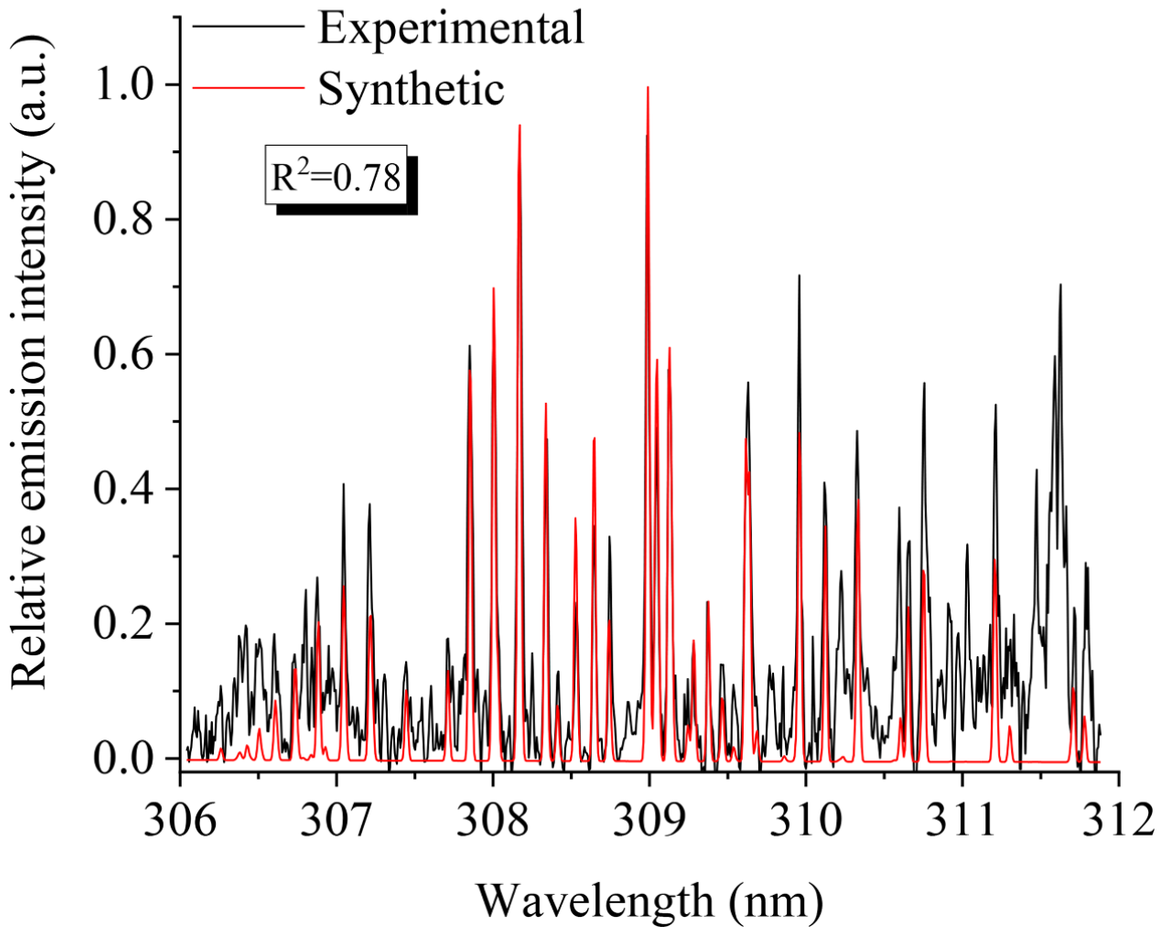

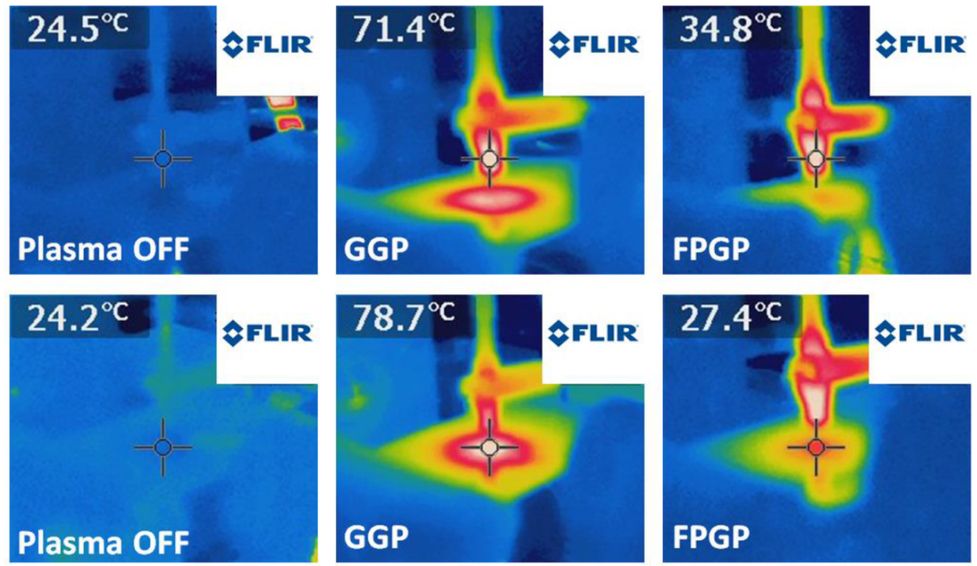

Figure 7. (Top) False-color IR camera images used to evaluate T_{Quartz} (upper images) and T_{Plate} (lower images), when using a floating-potential glass plate (FPGP, right column) and a grounded glass plate (GGP, middle column). Images on the left column refer to the case where the plasma was 'OFF'. (Bottom) Comparison between an experimental (black) and a synthetic (red) rotational spectra of the OH(A–X) used for the evaluation of T_{Rot} of OH(A), when using a GGP.

J. Phys. D: Appl. Phys. 53 (2020) 475202

Nanosecond pulsed argon plasma jet: temperatures

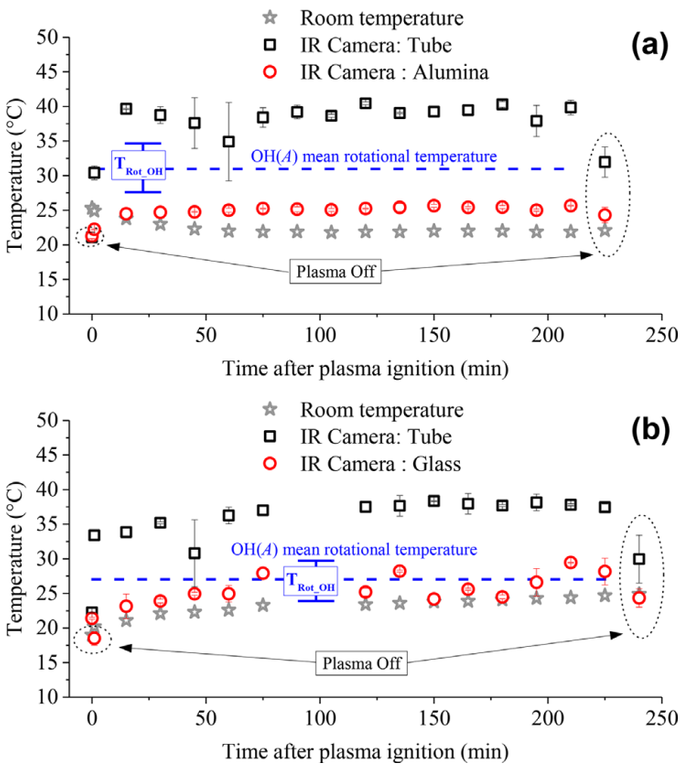

FIGURE 8 Temporal evolution (after the ignition of the plasma) of the temperature of the reactor's tube (T_{Quartz}, black squares in [a] and [b]) and of the dielectric targets (red circles, [a]-alumina [$T_{Alumina}$] and [b]-glass [T_{Glass}]). The gray stars refer to the room temperature (T_{Room}). The blue dashed lines correspond to the T_{rot} of OH(A) in the APPJ ($\sim T_{Gas}$, average value and standard deviation from 3 axial positions, see Figure 1). $V_p = 6$ kV, $f = 20$ kHz, $Q = 0.3$ l min^{-1}

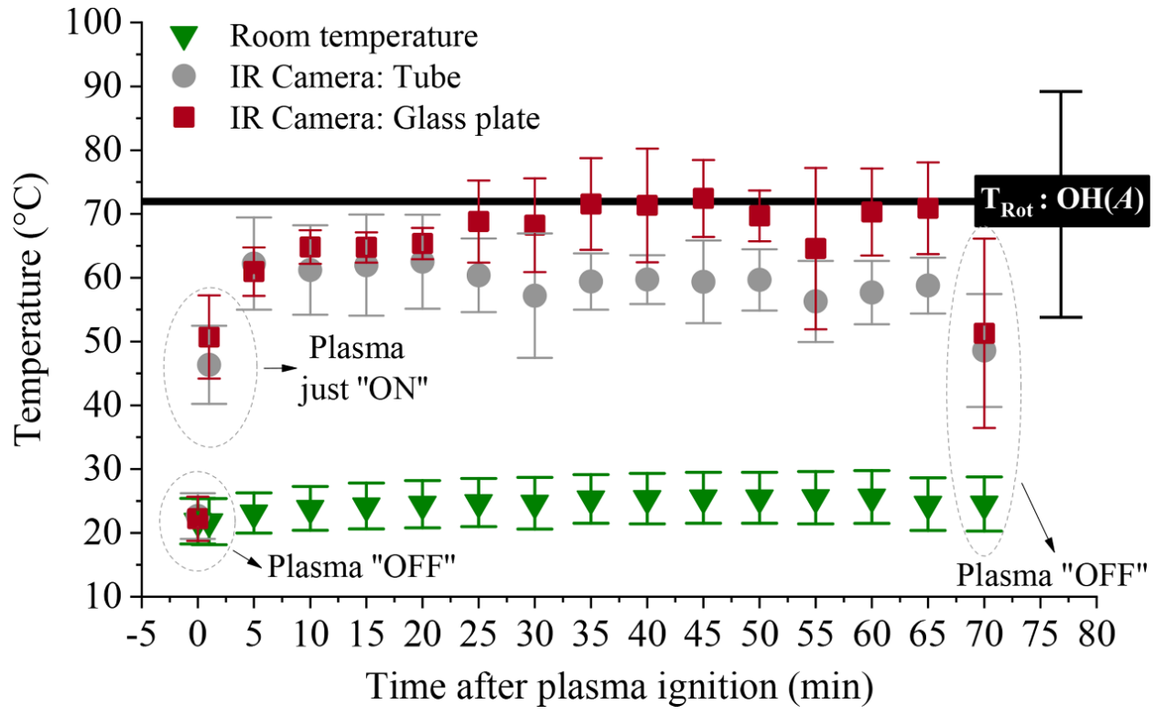

Figure 6. Temporal evolution, after the ignition of the plasma, of the temperatures of the capillary tube (T_{Quartz}; grey circles) and the glass plate (T_{Plate}, red squares) in the case of a grounded plate. The green triangles refer to the room temperature (T_{Room}). The thick black line refers to the average value of T_{Rot} of OH(A) (the black caps indicate the standard deviation). Values of T_{Room}, T_{Quartz} and T_{Plate} refer to four series, while T_{Rot} refers to three series of experiments performed in different dates. In each series, T_{Rot} was measured frequently during plasma operation (similarly to T_{Room}, T_{Quartz} and T_{Plate}).

Plasma Process Polym. 2018; e1800080
J. Phys. D: Appl. Phys. 53 (2020) 475202

Nanosecond pulsed argon plasma jet: desorption

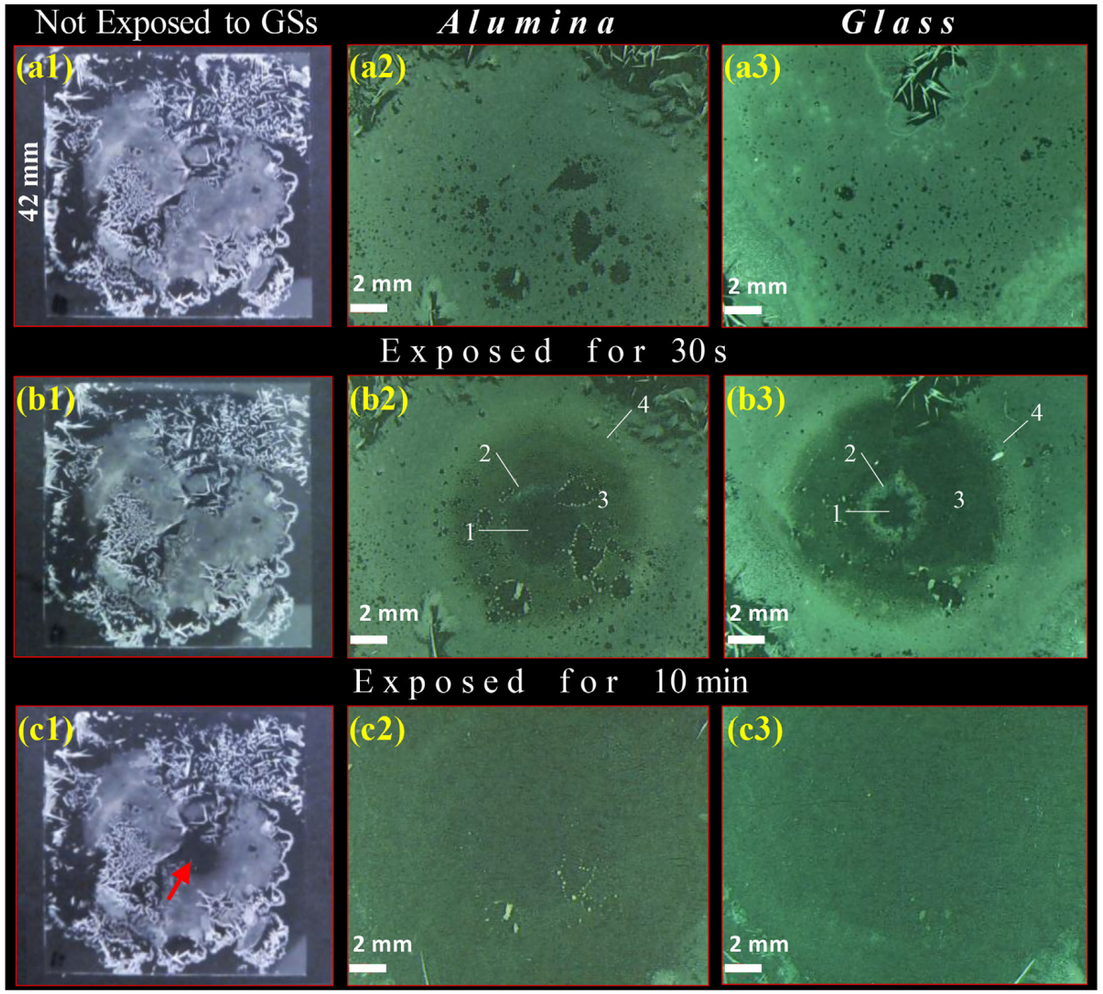

FIGURE 7 Images (b1) and (c1): high definition images of bibenzyl molecules deposited on a glass lamella ($42 \times 42 \times 0.2$ mm) and treated only by the gas flow. The effect of the plasma (see white numbers/lines) is shown in images (b2) and (c2) (alumina target) and (b3) and (c3) (glass target). The corresponding control specimens (before exposure) are shown in images (a1), (a2), and (a3). The deposits were exposed to the gas/plasma for 30 s ((b1), (b2), and (b3)) and 10 min ((c1), (c2), and (c3)). $V_p = 6$ kV, $f = 20$ kHz, $Q = 0.3\,\mathrm{l\,min^{-1}}$

Plasma Process Polym. 2018; e1800080

Nanosecond pulsed argon plasma jet: desorption

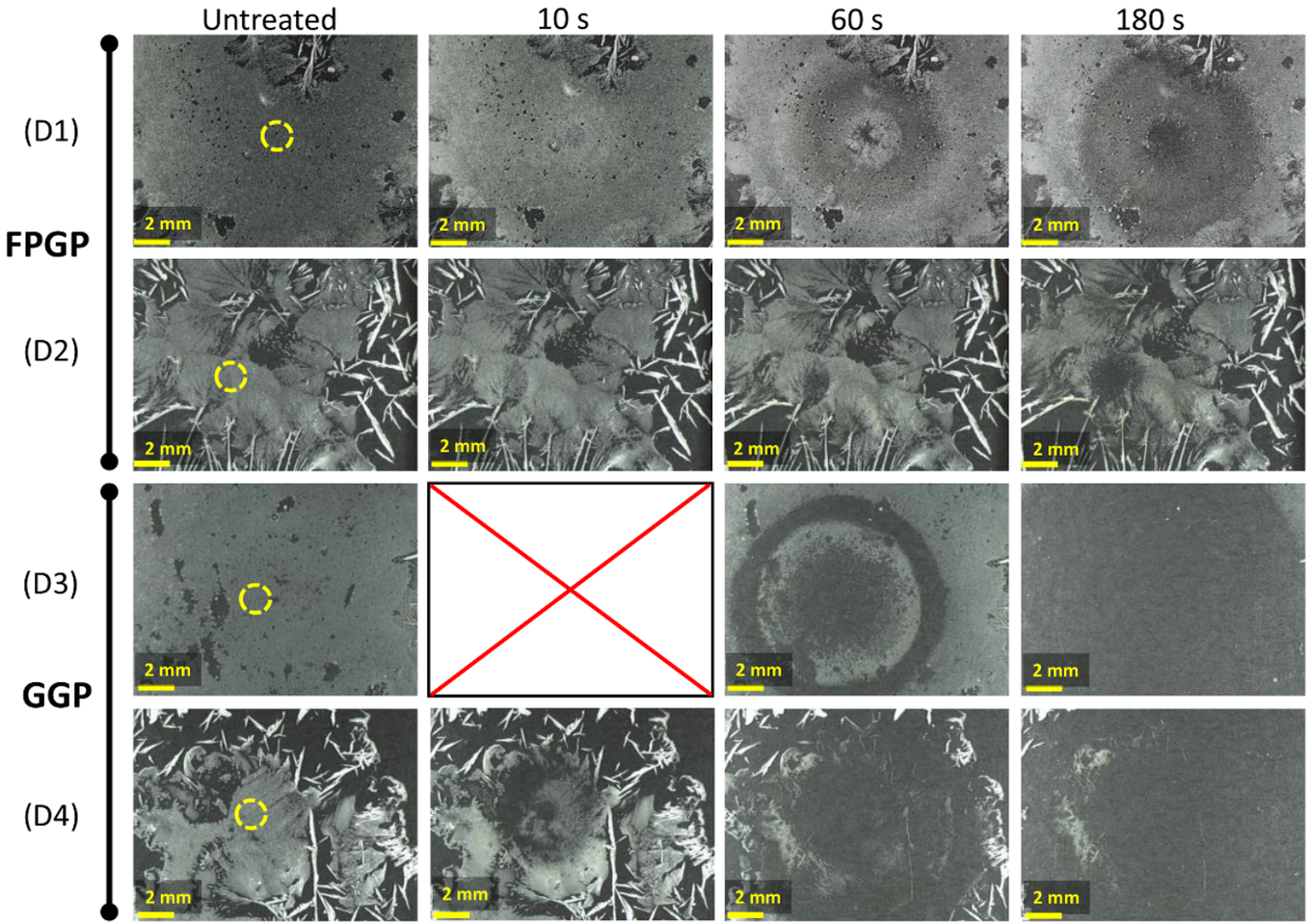

Figure 8. D1–D4: high-resolution grey-scale stereomicroscope images of resistant bibenzyl deposits exposed to the Ar APPJ 3 days after their preparation (exposure times applied: 10−180 s). D1 and D2 are two different deposits treated in the case of a floating-potential glass plate (FPGP), while D3 and D4 are another two deposits treated in the case of a grounded glass plate (GGP).

J. Phys. D: Appl. Phys. 53 (2020) 475202

Nanosecond pulsed argon plasma jet: desorption

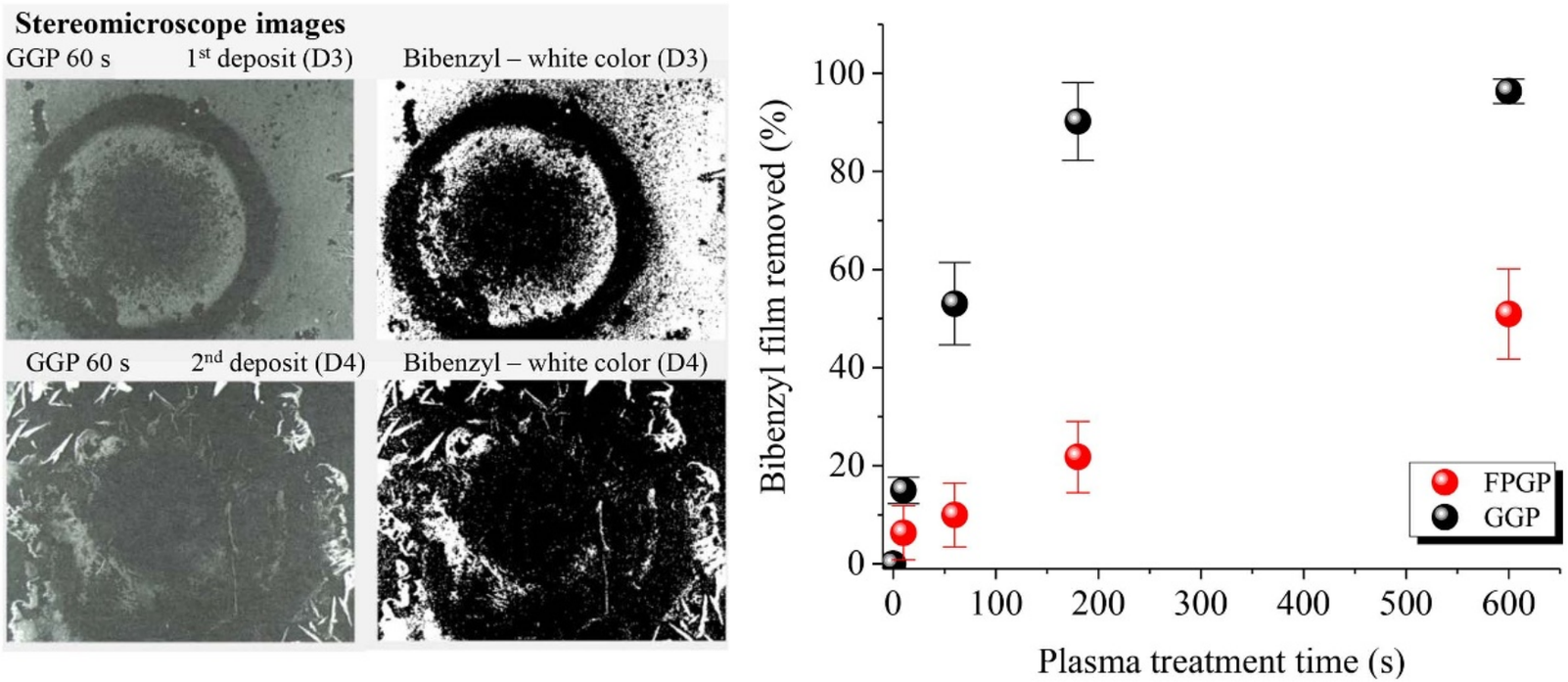

Figure 9. (Left) Digital processing results (right column) of the experimental images (left column) of the deposits D3 and D4 shown in figure 8 and plasma-treated for 60 s while using a grounded glass plate (GGP). (Right) Calculated percentage of bibenzyl film removed from the lamella surface as a function of the plasma treatment time for both electric potential conditions of the glass plate (obtained from all deposits of figure 8).

J. Phys. D: Appl. Phys. 53 (2020) 475202

Nanosecond pulsed argon plasma jet: desorption

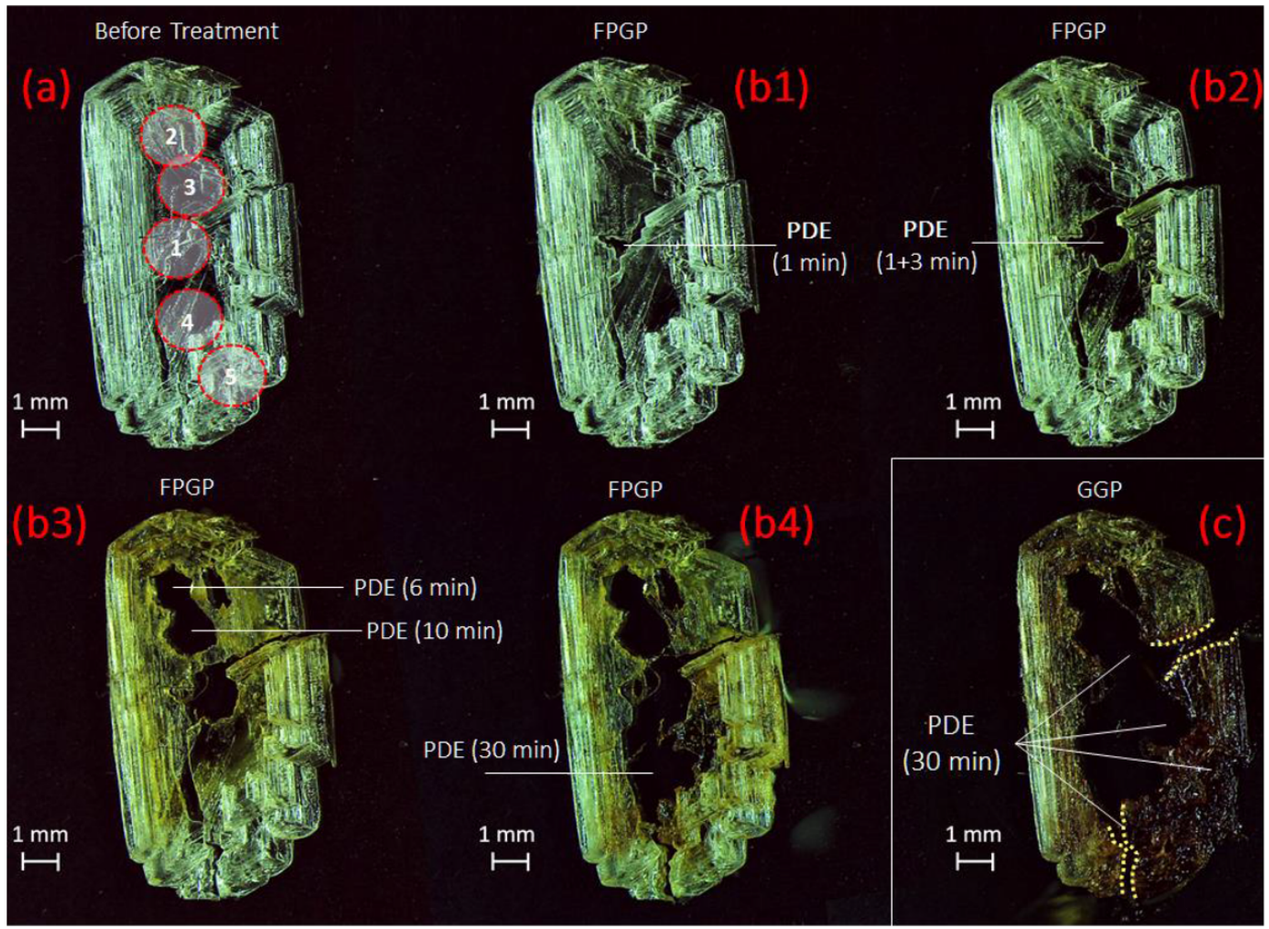

J. Phys. D: Appl. Phys. 53 (2020) 475202

Figure 10. High-resolution true-color stereomicroscope images showing the structural modification of a thick bibenzyl deposit after its exposure to the APPJ under floating-potential (FPGP, (b1)–(b4)) and grounded (GGP, (c)) electric potential conditions of the glass plate. (b) FPGP case: plasma applied (b1) for 1 min, and, then, (b2) for another 3 min at the 1st treated zone (i.e. circle 1 in (a)), (b3) for 6 min at the 2nd zone (circle 2 in (a)), (b3) for 10 min at the 3rd zone (circle 3 in (a)) and (b4) for 30 min at the 4th zone (circle 4 in (a)). (c) GGP case: plasma applied for 30 min at the 5th treated zone (circle 5 in (a)). PDE: Plasma desorption efficacy.

Conclusions

- **a ns-pulsed Ar APPJ was studied for the fast desorption of resistant bibenzyl deposits placed on glass** (at floating-potential or grounded directly) **and alumina plates**
- **maximum radial densities of the Ar($1s_5$) of up to 4×10^{14} cm^{-3} were measured at the centre of the APPJ**
- **the profile of the maximum radial density of Ar($1s_5$) was slightly wider for a grounded glass plate**
- **the Plasma Desorption Efficacy (PDE) was well demonstrated both on thin and thick bibenzyl deposits**, depending on the exposure time to the APPJ, but it was **much higher and faster for a grounded glass plate**
- **the bibenzyl removal was attributed to a combined action of Ar($1s_5$) metastables with oxidative species** (such as atomic oxygen, hydroxyl radical and ozone) **and ions** (such as N_4^+, Ar^+ and Ar_2^+)
- **thermal effects might also play a synergistic role but only in the case of a glass grounded plate**
- **this APPJ can be, therefore, adopted in various fields related to the fast desorption of weakly volatile organic compounds from different surfaces**
- **particularly, its joint use with Mass Spectrometry** (e.g. detection of prohibited substances such as explosives and drugs) **seems to be very promising for public-security applications**

Eur. Phys. J. Appl. Phys. (2016) 75: 24713
DOI: 10.1051/epjap/2016150594

THE EUROPEAN PHYSICAL JOURNAL APPLIED PHYSICS

Regular Article

Impact of an atmospheric argon plasma jet on a dielectric surface and desorption of organic molecules*

Xavier Damany, Stéphane Pasquiers[a], Nicole Blin-Simiand, Gérard Bauville, Blandine Bournonville, Michel Fleury, Pascal Jeanney, and João Santos Sousa

LPGP, CNRS, Univ. Paris-Sud, Univ. Paris-Saclay, 91405 Orsay Cedex, France

Received: 1 December 2015 / Received in final form: 9 March 2016 / Accepted: 26 April 2016

Journal of Applied Physics ARTICLE scitation.org/jou

Spatio-temporal distribution of absolute densities of argon metastable $1s_5$ state in the diffuse area of an atmospheric pressure nanosecond pulsed argon microplasma jet propagating into ambient air

Cite as: J. Appl. Phys. **126**, 073302 (2019); doi: 10.1063/1.5096407
Submitted: 17 March 2019 · Accepted: 20 July 2019 ·
Published Online: 19 August 2019

View Online Expo

Et. Es-sebbar,[a),b)] G. Bauville, M. Fleury, S. Pasquiers,[c)] and J. Santos Sousa[d)]

AFFILIATIONS

LPGP, CNRS, Univ. Paris-Sud, Université Paris-Saclay, 91045 Orsay, France

IOP Publishing Plasma Sources Science and Technology

Plasma Sources Sci. Technol. **27** (2018) 065003 (22pp) https://doi.org/10.1088/1361-6595/aac5b3

Effect of the gas flow rate on the spatiotemporal distribution of $Ar(1s_5)$ absolute densities in a ns pulsed plasma jet impinging on a glass surface

K Gazeli, G Bauville, M Fleury, P Jeanney, O Neveu, S Pasquiers[1] and J Santos Sousa[1]

LPGP, CNRS, Univ. Paris-Sud, Université Paris-Saclay, 91405 Orsay, France

E-mail: kristaq.gazeli@u-psud.fr, stephane.pasquiers@u-psud.fr and joao.santos-sousa@u-psud.fr

Received 18 December 2017, revised 2 May 2018
Accepted for publication 17 May 2018
Published 7 June 2018

CrossMark

Received: 18 April 2018 | Revised: 13 July 2018 | Accepted: 18 July 2018
DOI: 10.1002/ppap.201800080

FULL PAPER

PLASMA PROCESSES AND POLYMERS

$Ar(1s_5)$ absolute radial densities in a ns-pulsed argon plasma jet impinging on dielectric targets at floating potential – plasma action on organic molecules

Kristaq Gazeli | **Thomas Vazquez** | **Sara Al-Homsi** | **Gérard Bauville** | **Nicole Blin-Simiand** | **Blandine Bournonville** | **Michel Fleury** | **Pascal Jeanney** | **Olivier Neveu** | **Stéphane Pasquiers** | **João Santos Sousa**

LPGP, CNRS, Univ. Paris-Sud, Université Paris-Saclay, 91405 Orsay, France

Correspondence
Kristaq Gazeli, Stéphane Pasquiers, and João Santos Sousa, LPGP, CNRS, Univ. Paris-Sud, Université Paris-Saclay, 91405 Orsay, France.
Email: kristaq.gazeli@u-psud.fr (K.G.), stephane.pasquiers@u-psud.fr (S.P.), joao.santos-sousa@u-psud.fr (J.S.S.)

Funding information
Agence Nationale de la Recherche, Grant number: ANR-2013-SECU-0002-03

The present work is devoted to the precise spatiotemporal mapping of the absolute density of $Ar(1s_5)$ in a ns-pulsed argon plasma jet. The plasma impinges on glass and alumina targets at floating potential placed 5 mm away from the reactor's nozzle. Under these conditions, diffuse discharges are established in the small gas gap. As so, the line-of-sight absolute density of $Ar(1s_5)$ is effectively evaluated via laser absorption spectroscopy. The application of the Abel-inversion is also demonstrated for different operating conditions leading to the precise radial mapping of the $Ar(1s_5)$ absolute density. The influence of each target is studied for two gas flow rates, 0.3 and 0.4 l min^{-1}. The temporal density profiles over a voltage pulse period reveal two maxima related with the $Ar(1s_5)$ production in the streamer head and in the residual diffuse plasma channel. Furthermore, the maximum $Ar(1s_5)$ axial/radial density ($\sim 10^{13} - 3.5 \times 10^{14}$ cm^{-3}) depends on the target material and gas flow rate. Finally, the plasma is proved to be very effective for the fast desorption of organic molecules (bibenzyl) deposited on both targets. The results obtained suggest that the desorption of bibenzyl is due to the production of high $Ar(1s_5)$ densities at the close vicinity of the targets.

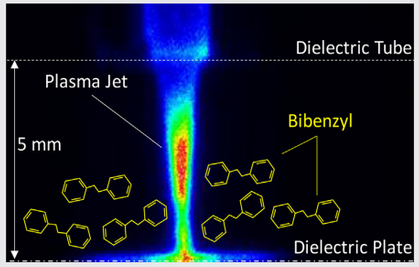

KEYWORDS
argon metastables, argon plasma jet, dielectric targets, laser absorption spectroscopy, organic substances, physical and chemical desorption, volatile organic compounds

IOP Publishing
Journal of Physics D: Applied Physics
J. Phys. D: Appl. Phys. **53** (2020) 475202 (26pp)
https://doi.org/10.1088/1361-6463/aba870

Experimental investigation of a ns-pulsed argon plasma jet for the fast desorption of weakly volatile organic compounds deposited on glass substrates at variable electric potential

K Gazeli, T Vazquez, G Bauville, N Blin-Simiand, B Bournonville, S Pasquiers and J Santos Sousa

Université Paris-Saclay, CNRS, Laboratoire de Physique des Gaz et des Plasmas, 91405 Orsay, France

E-mail: kristaq.gazeli@universite-paris-saclay.fr, stephane.pasquiers@universite-paris-saclay.fr and joao.santos-sousa@universite-paris-saclay.fr

Received 3 February 2020, revised 9 July 2020
Accepted for publication 22 July 2020
Published 1 September 2020

CrossMark

Special thanks to colleagues at the LPGP:

- **Thibault Darny**
- **Kristaq Gazeli**
- Gérard Bauville
- Michel Fleury
- Pascal Jeanney
- Nicole Blin-Simiand
- Stéphane Pasquiers

This research was funded by:

- the French *Agence Nationale de la Recherche* (***ANR***) through the ***PLASPAMS*** project (grant No. ANR-2013-SECU-0002-03)

- the French *Institut National du Cancer* (***INCa***) through the ***PLASCANCER*** project (INCa-PlanCancer no.17CP087-00)

- the **CNRS**

For more details:

Eur. Phys. J. Appl. Phys. (2016) 75: 24713 (https://doi.org/10.1051/epjap/2016150594)

Plasma Sources Sci. Technol. 27 (2018) 065003 (https://doi.org/10.1088/1361-6595/aac5b3)

Plasma Process Polym. 2018; e1800080 (https://doi.org/10.1002/ppap.201800080)

J. Appl. Phys. 126, 073302 (2019) (https://doi.org/10.1063/1.5096407)

J. Phys. D: Appl. Phys. 53 (2020) 475202 (https://doi.org/10.1088/1361-6463/aba870)

Plasma Sources Sci. Technol. 30 (2021) 105021 (https://doi.org/10.1088/1361-6595/ac2a18)

Thank you for your attention!